JOURNAL OF AGRICULTURAL AND FOOD CHEMISTRY

pubs.acs.org/JAFC Article

Fragmenlt Recombination Design, Synthesis, and Safener Activity of Novel Ester-Substituted Pyrazole Derivatives

Ling Jia,[#] Shuang Gao,[#] Yuan-Yuan Zhang, Li-Xia Zhao, Ying Fu,* and Fei Ye*

Cite This: *J. Agric. Food Chem.* 2021, 69, 8366–8379 Read Online

ACCESS | Metrics & More | Article Recommendations | Supporting Information

ABSTRACT: Fenoxaprop-*p*-ethyl (FE), a type of acetyl-CoA carboxylase (ACCase) inhibitor, has been extensively applied to a variety of crop plants. It can cause damage to wheat (*Triticum aestivum*) even resulting in the death of the crop. On the prerequisite of not reducing herbicidal efficiency on target weed species, herbicide safeners selectively protect crops from herbicide injury. Based on fragment splicing, a series of novel substituted pyrazole derivatives was designed to ultimately address the phytotoxicity to wheat caused by FE. The title compounds were synthesized in a one-pot way and characterized *via* infrared spectroscopy, ^{1}H nuclear magnetic resonance, ^{13}C nuclear magnetic resonance, and high-resolution mass spectrometry. The bioactivity assay proved that the FE phytotoxicity to wheat could be reduced by most of the title compounds. The molecular docking model indicated that compound **IV-21** prevented fenoxaprop acid (FA) from reaching or acting with ACCase. The absorption, distribution, metabolism, excretion, and toxicity predictions demonstrated that compound **IV-21** exhibited superior pharmacokinetic properties to the commercialized safener mefenpyr-diethyl. The current work revealed that a series of newly substituted pyrazole derivatives presented strong herbicide safener activity in wheat. This may serve as a potential candidate structure to contribute to the further protection of wheat from herbicide injury.

KEYWORDS: *ester-substituted pyrazole derivatives, synthesis, bioassay, safener activity, molecular simulation*

INTRODUCTION

In the biosynthesis process of fatty acids, acetyl-CoA carboxylase (ACCase) exerts a significant impact on the sustaining function of biological organisms including bacteria, fungi, plants, humans, and animals.[1−3] ACCase catalyzes the formation of malonyl CoA, which plays an important role in the maintenance of cell functions during the biosynthesis of long-chain fatty acids.[4] Malonyl CoA is produced in two stages, starting with acetyl-CoA and CO_2 followed by being catalyzed by ACCase. First, the biotin carboxylase subunit of ACCase catalyzes the ATP-dependent carboxylation of biotin. Then, the carboxyltransferase subunit catalyzes the process of transferring an activated group containing carboxyl groups to its acceptor acetyl-CoA.[5] Any exogenous substance inhibits the production of malonyl CoA, thereby inhibiting the synthesis of fatty acids, resulting in an increased permeability of the cell membrane structure of monocotyledonous plants, damage to the membrane structure, and ultimately death of the plants. Therefore, ACCase is the target of a series of important herbicides including aryloxyphenoxypropionates (AOPPs), cyclohexanediones (CHDs), and phenylpyrazolines (DENs).[6] ACCase inhibitors are highly selective, conductive in plants, have a low toxicity and long-lasting effects, are safe for subsequent crops, and can effectively control annual or perennial gramineous weeds after seedlings.

Fenoxaprop-*p*-ethyl (FE), a typical AOPP herbicide, is an inner-absorption herbicide for postemergence treatment. It is applied to control annual grasses and some broad-leaf weeds in fields.[7,8] FE is transmitted to the meristem and root growth points through stem and leaf absorption and is then rapidly converted into free carboxylic acid-containing phenoxy groups, which destroys the physiological effect of the normal growth of weeds and gradually withers leaves. It is a highly selective stem and leaf treatment agent.[9,10] However, due to the long-term and widespread use of FE, crops suffer varying degrees of phytotoxicity.[11−13] The application of FE results in crop yellowing, crop growth inhibition, and even crop death in serious cases. To reduce damage to crops, many methods have been reported that incorporate the scientific management of crop rotation and cultivation and the research and development of new herbicides.[14,15] In addition, the use of herbicide safeners is also considered to be an efficient solution.[16−18]

Herbicide safeners, also known as herbicide detoxifiers, are chemicals that increase plant tolerance to herbicides without affecting weed control efficacy.[19,20] The phenomenon of herbicide safeners was first discovered in 1947, when Hoffmann accidentally observed that after treatment with 2-(2,4,6-trichlorophenoxy) acetic acid, no phytotoxicity occurred when the herbicide was exposed to 2,4-dichlorophenoxyacetic acid (2,4-D). As the phenomenon of a safener was discovered, the first herbicide safener, 1,8-naphthalic anhydride (NA), was created in the mid-20th century.[21] Afterward, nearly 20 commercial safeners, produced by agrochemical companies

Received: April 16, 2021
Revised: July 12, 2021
Accepted: July 13, 2021
Published: July 26, 2021

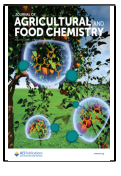

https://doi.org/10.1021/acs.jafc.1c02221
J. Agric. Food Chem. 2021, 69, 8366–8379

Scheme 1. Design of the New Fungicide Fluopyram

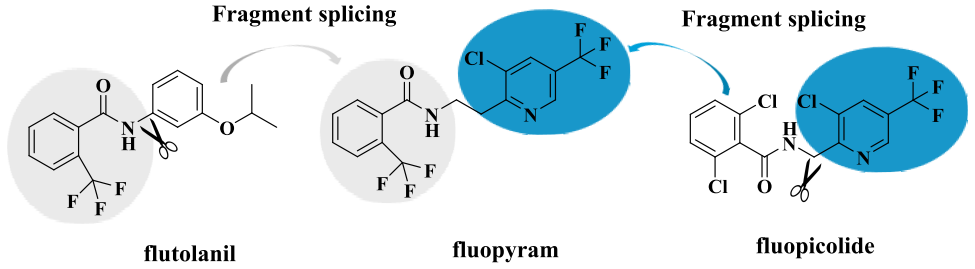

Scheme 2. Design of the Target Compounds

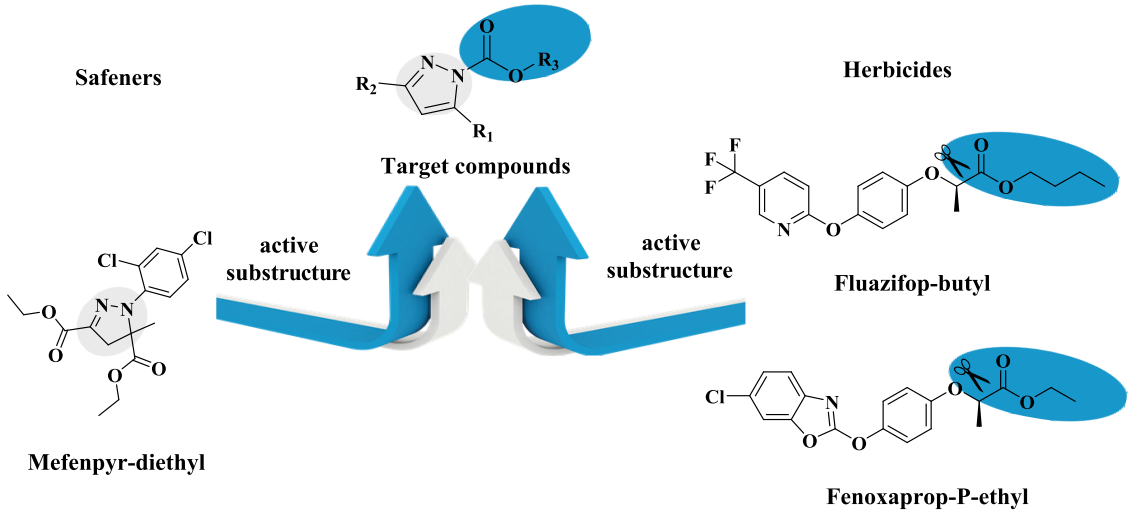

can be classified into diverse chemical families, including oxime ether derivatives, sulfonamides, dichloroacetamides, carboxylic acid derivatives, and phenyl pyrazoles.[22]

Studies have shown that herbicide safeners can elevate crop detoxification and metabolism by upregulating ATP-binding cassette (ABC) transporter proteins, glutathione S-transferases (GSTs), glutathione (GSH), and cytochrome P450 (CYP450), which counteract poison herbicides.[23,24] Mefenpyr-diethyl is an herbicide safener discovered by the Hoechst Company and belongs to the chemical category of phenyl pyrazoles. It was determined that it has a certain effect on preventing crops from herbicide damage.[25] In herbicide-tolerant wheat production systems, the combination of FE and mefenpyr-diethyl is an excellent method for weed control.[26,27] It is worth noting that a safener is treated as an "inert ingredient" in the USA, and there are few studies on its environmental behavior and toxicities. The usage of safeners is growing with the herbicide resistances. Commercial safeners have shown a series of risks to the environment.[28−30] To reduce the risk to the environment, it is necessary to design more safeners with a lower toxicity and higher activity. Therefore, research on safeners with a higher phenyl pyrazole activity is also more valuable. The research shows that delicate modifications to the structure of mefenpyr-diethyl will impact its biological activity, and it is determined that retaining the pyrazole heterocyclic group and ester group is the necessary chemical fragment for its safener activity.[25,31]

One of the main techniques for designing and optimizing novel framework structures with the target biological activity is the fragment splicing method. Many instances of fragment splicing have been demonstrated;[32−35] for example, the design of the novel fungicide fluopyram was formed by splicing the fragments of flutolanil and fluopicolide (Scheme 1).[36]

Over the past several years, some heterocyclic rings bearing N and O atom safeners have been found with excellent biological activities.[37−40] Based on our previous research,[41−45] the herbicide safener mefenpyr-diethyl was used as a precursor to splice the biologically active ester group structure of the herbicides fluazifop-butyl and fenoxaprop-*p*-ethyl with pyrazole compounds *via* amide bonds. A sequence of new ester-substituted pyrazole derivatives has been designed (Scheme 2). The title compounds were all characterized *via* infrared (IR) spectroscopy, ^{1}H nuclear magnetic resonance (^{1}H NMR), ^{13}C nuclear magnetic resonance (^{13}C NMR), and high-resolution mass spectrometry (HRMS) to characterize the accuracy of their structures. The safener activity of each compound was evaluated by measuring the growth index, ACCase activity, GST activity, and CYP450 content in wheat. The possible detoxification mechanism was determined, and novel effective safeners were designed through molecular structure comparisons and molecular docking. Furthermore, the pharmacokinetic properties of the compounds were evaluated through absorption, distribution, metabolism, excretion, and toxicity (ADMET) prediction. This research might provide an appropriate reference for the progress of more efficient pyrazole derivative herbicide safeners in the future.

MATERIALS AND METHODS

Instruments and Materials. All reagents were of analytical reagent grade, and no purification in later procedures was required (Table S1). The infrared (IR) spectra were recorded on an ALPHA-T (Bruker Corp., Billerica, MA, USA) infrared spectrophotometer using

https://doi.org/10.1021/acs.jafc.1c02221
J. Agric. Food Chem. 2021, 69, 8366−8379

potassium bromide pellets. Nuclear magnetic resonance (NMR) spectra were recorded on a Bruker AV400 spectrometer (Bruker Corp., Billerica, MA, USA), using deuterated chloroform as the solvent and tetramethylsilane (TMS) as an internal standard. The melting points were obtained using a Beijing Taike melting point apparatus (X-4; Beijing Taike, Beijing, China) and without corrections. The mass spectrum (HRMS; Bruker Corp., Billerica, MA, USA) was determined *via* high-resolution mass spectrometry. The X-ray diffraction data of the target compound were gathered on a Rigaku R-AXIS RAPID area-detector diffractometer (Rigaku Corp., Tokyo, Japan).

Preparation of Pyrazole Intermediates II.[46] 1,3-Dione (15 mmol) was dissolved in an anhydrous ethanol solution (50 mL) in a three-neck flask. Hydrazine hydrate (15 mmol) was added, and then, the mixture was incubated at 78 °C for 2 h. The solvent was removed under vacuum, and the crude products were purified *via* recrystallization with light petroleum ether and ethyl acetate to obtain the intermediate pyrazole **II**. Pyrazole intermediate **II** provided yields in the range of 73−88%.

General Procedure for Synthesis of Compounds IV-1−IV-35.[47] Compound **II** (7 mmol) and 50 mL of tetrahydrofuran were sequentially added to a three-neck flask. Subsequently, triethylamine (11 mmol) and acid chloride **III** (11 mmol) were added to the system. The next dropwise addition was complete, and the reaction was conducted under reflux for 1−1.5 h at 65 °C. After the reaction was complete (TLC monitoring), the mixture was washed three times with distilled water, and then, the organic phase was dried with anhydrous $MgSO_4$ for 0.5 h. Compound **IV** was then obtained at a yield rate of 33−87% after the solvent was removed under a reduced pressure, and the crude products were purified *via* column chromatography on a silica gel, eluted with ethyl acetate and petroleum ether (1:10−1:50) or recrystallized with ethyl acetate and light petroleum ether.

Isopropyl-3-methyl-5-phenyl-1H-pyrazole-1-carboxylate ***IV-1***. Light yellow oily liquid; yield: 73%; IR (KBr) ν (cm^{-1}): 3064−2880 (C−H), 1761 (O−C═O), 1572 (C═N); ^{1}H NMR (400 MHz, $CDCl_3$) δ (ppm): 7.91−6.47 (m, 6H, Ar−H), 5.29−5.23 (m, 1H, CH), 2.59 (s, 3H, CH_3), 1.48 (d, 6H, 2 × CH_3); ^{13}C NMR (100 MHz, $CDCl_3$) δ (ppm): 153.90, 150.17, 145.09, 132.03, 128.88, 128.88, 128.58, 128.58, 126.46, 107.71, 72.66, 21.83, 21.83, 14.68; HRMS (ESI): calcd for $C_{14}H_{17}N_2O_2$ ([M + H^+]), 245.1289; found, 245.1290.

Isopropyl-3,5-diphenyl-1H-pyrazole-1-carboxylate ***IV-2***. Light yellow oily liquid; yield: 65%; IR (KBr) ν (cm^{-1}): 3102−2877 (C−H), 1759 (O−C═O), 1562 (C═N); ^{1}H NMR (400 MHz, $CDCl_3$) δ (ppm): 7.94−6.69 (m, 10H, Ar−H), 5.13−5.06 (m, 1H, CH), 1.20 (d, J = 6.3 Hz, 6H, 2 × CH_3); ^{13}C NMR (100 MHz, $CDCl_3$) δ (ppm): 154.01, 149.45, 147.85, 131.75, 131.55, 129.11, 129.11, 129.05, 129.05, 128.74, 128.74, 128.65, 127.83, 126.48, 126.48, 108.96, 72.77, 21.40, 21.40; HRMS (ESI): calcd for $C_{19}H_{19}N_2O_2$ ([M + H^+]), 307.1446; found, 307.1447.

Isopropyl-5-phenyl-3-(trifluoromethyl)-1H-pyrazole-1-carboxylate ***IV-3***. Light yellow oily liquid; yield: 58%; IR (KBr) ν (cm^{-1}): 3057−2882 (C−H), 1775 (O−C═O), 1570 (C═N); ^{1}H NMR (400 MHz, $CDCl_3$) δ (ppm): 7.90−7.16 (m, 6H, Ar−H), 5.37−5.28 (m, 1H, CH), 1.49 (d, J = 6.3 Hz, 6H, 2 × CH_3); ^{13}C NMR (100 MHz, $CDCl_3$) δ (ppm): 153.42, 148.45, 147.48, 130.42, 129.73, 129.73, 128.09, 126.47, 120.58, 120.58, 110.76, 74.51, 21.49, 21.49; HRMS (ESI): calcd for $C_{14}H_{14}F_3N_2O_2$ ([M + H^+]), 321.0826; found, 321.0827.

Isopropyl-5-(p-tolyl)-3-(trifluoromethyl)-1H-pyrazole-1-carboxylate ***IV-4***. Light yellow oily liquid; yield: 52%; IR (KBr) ν (cm^{-1}): 3123−2874 (C−H), 1772 (O−C═O), 1568 (C═N); ^{1}H NMR (400 MHz, $CDCl_3$) δ (ppm): 7.77−7.13 (m, 5H, Ar−H), 5.35−5.29 (m, 1H, CH), 2.39 (s, 3H, CH_3), 1.47 (d, J = 6.3 Hz, 6H, 2 × CH_3); ^{13}C NMR (100 MHz, $CDCl_3$) δ (ppm): 153.48, 148.61, 147.54, 139.86, 129.57, 129.57, 128.99, 127.61, 126.37, 126.37, 120.64, 110.70, 74.41, 21.48, 21.48; HRMS (ESI): calcd for $C_{15}H_{16}F_3N_2O_2$ ([M + H^+]), 313.1162; found, 313.1164.

Isopropyl-5-(furan-2-yl)-3-(trifluoromethyl)-1H-pyrazole-1-carboxylate ***IV-5***. Orange oily liquid; yield: 47%; IR (KBr) ν (cm^{-1}): 3131−2989 (C−H), 1773 (O−C═O), 1547 (C═N); ^{1}H NMR (400 MHz, $CDCl_3$) δ (ppm): 7.53−6.52 (m, 4H, Ar−H), 5.29−5.23 (m, 1H, CH), 1.43 (d, J = 6.3 Hz, 6H, 2 × CH_3); ^{13}C NMR (100 MHz, $CDCl_3$) δ (ppm): 148.56, 143.85, 142.35, 138.75, 125.40, 121.66, 118.98, 113.52, 111.72, 74.47, 21.52, 21.52; HRMS (ESI): calcd for $C_{12}H_{12}F_3N_2O_3$ ([M + H^+]), 311.0621; found, 311.0614.

Isobutyl-3-methyl-5-phenyl-1H-pyrazole-1-carboxylate ***IV-6***. White solid; yield: 70%; m.p. 104.0−104.8 °C; IR (KBr) ν (cm^{-1}): 3107−2875 (C−H), 1748 (O−C═O), 1573 (C═N); ^{1}H NMR (400 MHz, $CDCl_3$) δ (ppm): 7.86−6.49 (m, 6H, Ar−H), 4.24 (d, J = 6.8 Hz, 2H, CH_2), 2.61 (s, 3H, CH_3), 2.22−2.16 (m, 1H, CH), 1.06 (d, J = 6.7 Hz, 6H, 2CH_3); ^{13}C NMR (100 MHz, $CDCl_3$) δ (ppm): 154.00, 150.75, 145.13, 131.97, 128.94, 128.94, 128.61, 126.41, 126.41,107.73, 73.93, 27.86, 19.11, 19.11, 14.59; HRMS (ESI): calcd for $C_{15}H_{19}N_2O_2$ ([M + H^+]), 259.1444; found, 259.1447.

Isobutyl-3,5-diphenyl-1H-pyrazole-1-carboxylate ***IV-7***. White solid; yield: 66%; m.p. 90.7−91.7 °C; IR (KBr) ν (cm^{-1}): 2967−2875 (C−H), 1767 (O−C═O), 1562 (C═N); ^{1}H NMR (400 MHz, $CDCl_3$) δ (ppm): 7.93−6.71 (m, 11H, Ar−H), 4.09 (d, J = 6.8 Hz, 2H, CH_2), 1.94−1.82 (m, 1H, CH), 0.82 (d, J = 6.7 Hz, 6H, 2 × CH_3); ^{13}C NMR (100 MHz, $CDCl_3$) δ (ppm): 154.16, 150.20, 147.98, 131.71, 131.34, 129.14, 129.14, 129.06, 128.88, 128.88, 128.71, 127.99, 127.99, 126.48, 126.48, 109.19, 74.21, 27.61, 18.83, 18.83; HRMS (ESI): calcd for $C_{20}H_{21}N_2O_2$ ([M + H^+]), 321.1606; found, 321.1603.

Isobutyl-5-phenyl-3-(trifluoromethyl)-1H-pyrazole-1-carboxylate ***IV-8***. White solid; yield: 62%; m.p. 41.2−41.7 °C; IR (KBr) ν (cm^{-1}): 2992−2896 (C−H), 1775 (O−C═O), 1571 (C═N); ^{1}H NMR (400 MHz, $CDCl_3$) δ (ppm): 7.88−7.18 (m, 6H, Ar−H), 4.31 (d, J = 6.8 Hz, 2H, CH_2), 2.23−2.16 (m, 1H, CH), 1.05 (d, J = 6.7 Hz, 6H, 2 × CH_3); ^{13}C NMR (100 MHz, $CDCl_3$) δ (ppm): 153.50, 148.29, 130.37, 129.79, 129.79, 128.90, 126.44, 126.44, 110.86, 110.83, 77.23, 75.32, 27.76, 18.90, 18.90; HRMS (ESI): calcd for $C_{15}H_{16}F_3N_2O_2$ ([M + H^+]), 313.1162; found, 313.1164.

Isobutyl-5-(p-tolyl)-3-(trifluoromethyl)-1H-pyrazole-1-carboxylate ***IV-9***. White solid; yield: 55%; m.p. 72.1−72.6 °C; IR (KBr) ν (cm^{-1}): 3117−2877 (C−H), 1776 (O−C═O), 1588 (C═N); ^{1}H NMR (400 MHz, $CDCl_3$) δ (ppm): 7.78−7.14 (m, 5H, Ar−H), 4.30 (d, J = 6.7 Hz, 2H, CH_2), 2.39 (s, 3H, CH_3), 2.21−2.15 (m, 1H, CH), 1.06 (d, J = 6.7 Hz, 6H, 2 × CH_3); ^{13}C NMR (100 MHz, $CDCl_3$) δ (ppm): 153.56, 149.28, 139.94, 129.59, 128.91, 127.55, 127.55, 126.76, 126.76, 120.55, 108.27, 75.26, 27.76, 21.42, 18.90, 18.90; HRMS (ESI): calcd for $C_{16}H_{18}F_3N_2O_2$ ([M + H^+]), 327.1323; found, 327.1320.

Isobutyl-5-(furan-2-yl)-3-(trifluoromethyl)-1H-pyrazole-1-carboxylate ***IV-10***. Orange oily liquid; yield: 40%; IR (KBr) ν (cm^{-1}): 3150−2880 (C−H), 1779 (O−C═O), 1554 (C═N); ^{1}H NMR (400 MHz, $CDCl_3$) δ (ppm): 7.53−6.52 (m, 4H, Ar−H), 4.25 (d, J = 6.9 Hz, 2H, CH_2), 2.17−2.10 (m, 1H, CH), 1.00 (d, J = 6.8 Hz, 6H, 2 × CH_3); ^{13}C NMR (100 MHz, $CDCl_3$) δ (ppm): 149.26, 144.00, 144.00, 142.33, 138.96, 121.64, 111.81, 109.59, 107.36, 75.20, 27.76, 18.86, 18.86; HRMS (ESI): calcd for $C_{13}H_{14}F_3N_2O_3$ ([M + H^+]), 303.0956; found, 303.0957.

Propyl-3-methyl-5-phenyl-1H-pyrazole-1-carboxylate ***IV-11***. White solid; yield: 87%; m.p. 70.2−70.6 °C; IR (KBr) ν (cm^{-1}): 3088−2832 (C−H), 1732 (O−C═O), 1576 (C═N); ^{1}H NMR (400 MHz, $CDCl_3$) δ (ppm): 7.78−6.43 (m, 6H, Ar−H), 4.35 (t, J = 6.9 Hz, 2H, CH_2), 2.54 (s, 3H, CH_3), 1.85−1.79 (m, 2H, CH_2), 0.99 (t, J = 7.4 Hz, 3H, CH_3); ^{13}C NMR (100 MHz, $CDCl_3$) δ (ppm): 154.06, 150.72, 145.30, 131.93, 128.94, 128.60, 128.60, 126.46, 126.46, 107.77, 69.61, 22.03, 14.74, 10.29; HRMS (ESI): calcd for $C_{14}H_{17}N_2O_2$ ([M + H^+]), 245.1286; found, 245.1285.

Propyl-3,5-diphenyl-1H-pyrazole-1-carboxylate ***IV-12***. White solid; yield: 82%; m.p. 89.3−90.0 °C; IR (KBr) ν (cm^{-1}): 3027−2832 (C−H), 1752 (O−C═O), 1599 (C═N); ^{1}H NMR (400 MHz, $CDCl_3$) δ (ppm): 7.93−6.71 (m, 11H, Ar−H), 4.27 (d, J = 13.6 Hz, 2H, CH_2), 1.67−1.62 (m, 2H, CH_2), 0.85 (t, J = 7.4 Hz, 3H, CH_3); ^{13}C NMR (100 MHz, $CDCl_3$) δ (ppm): 154.14, 150.13, 148.11,

https://doi.org/10.1021/acs.jafc.1c02221
J. Agric. Food Chem. 2021, 69, 8366−8379

131.70, 131.27, 129.12, 129.12, 129.06, 129.06, 128.86, 128.86, 128.69, 127.91, 127.91, 126.50, 109.16, 69.79, 21.74, 10.09; HRMS (ESI): calcd for $C_{19}H_{19}N_2O_2$ ([M + H$^+$]), 307.1442; found, 307.1441.

Propyl-5-phenyl-3-(trifluoromethyl)-1H-pyrazole-1-carboxylate ***IV-13***. White solid; yield: 78%; m.p. 50.0−50.7 °C; IR (KBr) ν (cm^{-1}): 3041−2861 (C−H), 1758 (O−C═O), 1561 (C═N); ^{1}H NMR (400 MHz, $CDCl_3$) δ (ppm): 7.89−7.18 (m, 6H, Ar−H), 4.48 (t, J = 6.8 Hz, 2H, CH_2), 1.94−1.85 (m, 2H, CH_2), 1.06 (t, J = 7.4 Hz, 3H, CH_3); ^{13}C NMR (100 MHz, $CDCl_3$) δ (ppm): 153.57, 130.33, 129.71, 129.55, 129.06, 128.91, 128.91, 128.17, 126.47, 126.47, 110.86, 71.00, 21.65, 10.00; HRMS (ESI): calcd for $C_{14}H_{14}F_3N_2O_2$ ([M + H$^+$]), 299.1003; found, 299.1002.

Propyl-5-(p-tolyl)-3-(trifluoromethyl)-1H-pyrazole-1-carboxylate ***IV-14***. White solid; yield: 70%; m.p. 42.0−42.8 °C; IR (KBr) ν (cm^{-1}): 2952−2860 (C−H), 1761 (O−C═O), 1605 (C═N); ^{1}H NMR (400 MHz, $CDCl_3$) δ (ppm): 7.78−7.14 (m, 5H, Ar−H), 4.47 (t, J = 6.8 Hz, 2H, CH_2), 2.39 (s, 3H, CH_3), 1.92−1.85 (m, 2H, CH_2), 1.05 (t, J = 7.4 Hz, 3H, CH_3); ^{13}C NMR (100 MHz, $CDCl_3$) δ (ppm): 1149.24, 148.84, 145.17, 139.70, 128.94, 128.94, 128.94, 128.86, 128.86, 126.70, 108.26, 70.66, 21.70, 21.41, 9.99; HRMS (ESI): calcd for $C_{15}H_{16}F_3N_2O_2$ ([M + H$^+$]), 313.1156; found, 313.1158.

Propyl-5-(furan-2-yl)-3-(trifluoromethyl)-1H-pyrazole-1-carboxylate ***IV-15***. Light yellow oily liquid; yield: 64%; IR (KBr) ν (cm^{-1}): 3125−2862 (C−H), 1765 (O−C═O), 1495 (C═N); ^{1}H NMR (400 MHz, $CDCl_3$) δ (ppm): 7.53−6.52 (m, 4H, Ar−H), 4.48 (t, J = 6.9 Hz, 2H, CH_2), 1.93−1.81 (m, 2H, CH_2), 1.04 (t, J = 7.4 Hz, 3H, CH_3); ^{13}C NMR (100 MHz, $CDCl_3$) δ (ppm): 148.07, 145.76, 143.76, 120.35, 117.68, 113.83, 111.86, 110.60, 109.66, 71.11, 21.79, 10.08; HRMS (ESI): calcd for $C_{12}H_{12}F_3N_2O_3$ ([M + H$^+$]), 289.0800; found, 289.0799.

Butyl-3-methyl-5-phenyl-1H-pyrazole-1-carboxylate ***IV-16***. White solid; yield: 81%; m.p. 46.4−46.8 °C; IR (KBr) ν (cm^{-1}): 3111−2873 (C−H), 1750 (O−C═O), 1573 (C═N); ^{1}H NMR (400 MHz, $CDCl_3$) δ (ppm): 7.85−6.49 (m, 6H, Ar−H), 4.46 (t, J = 6.9 Hz, 2H, CH_2), 2.60 (s, 3H, CH_3), 1.84 (m, 2H, CH_2), 1.54−1.45 (m, 2H, CH_2), 1.00 (t, J = 7.4 Hz, 3H, CH_3); ^{13}C NMR (100 MHz, $CDCl_3$) δ (ppm): 154.04, 150.75, 145.29, 131.94, 128.94, 128.60, 128.60, 126.44, 126.44, 107.73, 67.96, 30.63, 19.06, 14.52, 13.72; HRMS (ESI): calcd for $C_{15}H_{19}N_2O_2$ ([M + H$^+$]), 259.1443; found, 259.1441.

Butyl-3,5-diphenyl-1H-pyrazole-1-carboxylate ***IV-17***. White solid; yield: 76%; m.p. 104.3−104.5 °C; IR (KBr) ν (cm^{-1}): 3048−2870 (C−H), 1766 (O−C═O), 1562 (C═N); ^{1}H NMR (400 MHz, $CDCl_3$) δ (ppm): 7.92−6.71 (m, 11H, Ar−H), 4.31 (t, J = 6.7 Hz, 2H, CH_2), 1.59 (m, 2H, CH_2), 1.29−1.20 (m, 2H, CH_2), 0.87 (t, J = 7.4 Hz, 3H, CH_3); ^{13}C NMR (100 MHz, $CDCl_3$) δ (ppm): 154.20, 150.15, 148.10, 131.71, 131.30, 129.15, 129.15, 129.08, 129.08, 128.85, 128.85, 127.92, 127.92, 126.51, 126.51, 109.18, 68.16, 30.33, 18.87, 13.63; HRMS (ESI): calcd for $C_{20}H_{21}N_2O_2$ ([M + H$^+$]), 321.1595; found, 321.1598.

(Trifluoromethyl)-1H-pyrazole-1-carboxylate ***IV-18***. White solid; yield: 70%; m.p. 43.2−44.1 °C; IR (KBr) ν (cm^{-1}): 3080−2865 (C−H), 1775 (O−C═O), 1572 (C═N); ^{1}H NMR (400 MHz, $CDCl_3$) δ (ppm): 7.53−7.17 (m, 6H, Ar−H), 4.52 (t, J = 6.8 Hz, 2H, CH_2), 1.85 (m, 2H, CH_2), 1.52−1.43 (m, 2H, CH_2), 1.00 (t, J = 7.4 Hz, 3H, CH_3); ^{13}C NMR (100 MHz, $CDCl_3$) δ (ppm): 153.55, 148.24, 130.36, 129.79, 129.05, 128.89, 128.89, 128.14, 126.46, 126.46, 110.83, 69.33, 30.36, 18.87, 13.63; HRMS (ESI): calcd for $C_{15}H_{16}F_3N_2O_2$ ([M + H$^+$]), 313.1160; found, 313.1158.

Butyl-5-(p-tolyl)-3-(trifluoromethyl)-1H-pyrazole-1-carboxylate ***IV-19***. White solid; yield: 66%; m.p. 76.4−77.0 °C; IR (KBr) ν (cm^{-1}): 2966−2878 (C−H), 1775 (O−C═O), 1602 (C═N); ^{1}H NMR (400 MHz, $CDCl_3$) δ (ppm): 7.33−6.59 (m, 5H, Ar−H), 4.34 (t, J = 6.7 Hz, 2H, CH_2), 2.41 (s, 3H, CH_3), 1.68−1.54 (m, 2H, CH_2), 1.30−1.20 (m, 2H, CH_2), 0.88 (t, J = 7.4 Hz, 3H, CH_3); ^{13}C NMR (100 MHz, $CDCl_3$) δ (ppm): 149.22, 148.78, 145.55, 145.17, 139.68, 128.85, 128.85, 126.74, 121.79, 119.03, 108.25, 69.07, 30.26, 21.40, 18.80, 13.58; HRMS (ESI): calcd for $C_{16}H_{18}F_3N_2O_2$ ([M + H$^+$]), 327.1319; found, 327.1315.

Butyl-5-(furan-2-yl)-3-(trifluoromethyl)-1H-pyrazole-1-carboxylate ***IV-20***. White solid; yield: 54%; m.p. 33.9−34.5 °C; IR (KBr) ν (cm^{-1}): 3145−2930 (C−H), 1776 (O−C═O), 1507 (C═N); ^{1}H NMR (400 MHz, $CDCl_3$) δ (ppm): 7.53−6.52 (m, 4H, Ar−H), 4.52 (t, J = 6.9 Hz, 2H, CH_2), 1.88−1.81 (m, 2H, CH_2), 1.52−1.43 (m, 2H, CH_2), 0.99 (t, J = 7.4 Hz, 3H, CH_3); ^{13}C NMR (100 MHz, $CDCl_3$) δ (ppm): 148.07, 145.88, 143.74, 143.74, 111.84, 111.84, 110.61, 109.63, 109.63, 69.48, 30.34, 18.83, 13.63; HRMS (ESI): calcd for $C_{13}H_{14}F_3N_2O_3$ ([M + H$^+$]), 303.0957; found, 303.0953.

2-Chloroethyl-3-methyl-5-phenyl-1H-pyrazole-1-carboxylate ***IV-21***. Light yellow oily liquid; yield: 65%; IR (KBr) ν (cm^{-1}): 3109−2890 (C−H), 1751 (O−C═O), 1572 (C═N); ^{1}H NMR (400 MHz, $CDCl_3$) δ (ppm): 7.90−6.51 (m, 6H, Ar−H), 4.69 (t, J = 6.0 Hz, 2H, CH_2), 3.87 (t, J = 6.0 Hz, 2H, CH_2), 2.61 (d, J = 1.0 Hz, 3H, CH_3); ^{13}C NMR (100 MHz, $CDCl_3$) δ (ppm): 154.59, 150.19, 145.60, 131.67, 129.14, 128.65, 128.65, 126.48, 126.48, 108.15, 66.86, 40.80, 14.51; HRMS (ESI): calcd for $C_{13}H_{14}ClN_2O_2$ ([M + H$^+$]), 265.0746; found, 265.0744.

2-Chloroethyl-3,5-diphenyl-1H-pyrazole-1-carboxylate ***IV-22***. White solid; yield: 57%; m.p. 122.9−123.3 °C; IR (KBr) ν (cm^{-1}): 3057−2952 (C−H), 1763 (O−C═O), 1564 (C═N); ^{1}H NMR (400 MHz, $CDCl_3$) δ (ppm): 7.97−6.74 (m, 11H, Ar−H), 4.54 (t, J = 6.0 Hz, 2H, CH_2), 3.65 (t, J = 6.0 Hz, 2H, CH_2); ^{13}C NMR (100 MHz, $CDCl_3$) δ (ppm): 154.73, 149.70, 148.47, 131.46, 130.93, 129.36, 129.14, 129.14, 129.08, 129.08, 128.78, 128.78, 128.00, 123.57, 126.57, 109.62, 67.03, 40.48; HRMS (ESI): calcd for $C_{18}H_{16}ClN_2O_2$ ([M + H$^+$]), 327.0900; found, 327.0900.

2-Chloroethyl-5-phenyl-3-(trifluoromethyl)-1H-pyrazole-1-carboxylate ***IV-23***. Light yellow oily liquid; yield: 54%; IR (KBr) ν (cm^{-1}): 3125−2884 (C−H), 1776 (O−C═O), 1574 (C═N); ^{1}H NMR (400 MHz, $CDCl_3$) δ (ppm): 7.93−7.21 (m, 6H, Ar−H), 4.75 (t, J = 5.9 Hz, 2H, CH_2), 3.88 (t, J = 5.9 Hz, 2H, CH_2); ^{13}C NMR (100 MHz, $CDCl_3$) δ (ppm): 154.05, 147.85, 130.10, 128.96, 128.96, 126.52, 126.52, 125.72, 120.40, 117.72, 113.34, 68.05, 40.34; HRMS (ESI): calcd for $C_{13}H_{11}ClF_3N_2O_2$ ([M + H$^+$]), 319.0461; found, 319.0463.

2-Chloroethyl-5-(p-tolyl)-3-(trifluoromethyl)-1H-pyrazole-1-carboxylate ***IV-24***. White solid; yield: 43%; m.p. 77.4−78.0 °C; IR (KBr) ν (cm^{-1}): 3154−2923 (C−H), 1772 (O−C═O), 1528 (C═N); ^{1}H NMR (400 MHz, $CDCl_3$) δ (ppm): 7.84−7.17 (m, 5H, Ar−H), 4.74 (t, J = 6.0 Hz, 2H, CH_2), 3.87 (t, J = 6.0 Hz, 2H, CH_2), 2.40 (s, 3H, CH_3); ^{13}C NMR (100 MHz, $CDCl_3$) δ (ppm): 154.10, 147.89, 140.19, 129.65, 129.65, 127.29, 126.42, 126.42, 120.44, 117.76, 111.28, 67.98, 40.35, 21.42; HRMS (ESI): calcd for $C_{14}H_{13}ClF_3N_2O_2$ ([M + H$^+$]), 333.0618; found, 333.0607.

2-Chloroethyl-5-(furan-2-yl)-3-(trifluoromethyl)-1H-pyrazole-1-carboxylate ***IV-25***. Light yellow oily liquid; yield: 38%; IR (KBr) ν (cm^{-1}): 3148−2966 (C−H), 1784 (O−C═O), 1506 (C═N); ^{1}H NMR (400 MHz, $CDCl_3$) δ (ppm): 7.54−6.53 (m, 4H, Ar−H), 4.75 (t, J = 6.0 Hz, 2H, CH_2), 3.87 (t, J = 6.0 Hz, 2H, CH_2); ^{13}C NMR (100 MHz, $CDCl_3$) δ (ppm): 147.71, 146.28, 145.51, 143.97, 120.24, 117.56, 111.92, 111.05, 110.04, 68.11, 40.26; HRMS (ESI): calcd for $C_{11}H_9ClF_3N_2O_3$ ([M + H$^+$]), 309.0254; found, 309.0250.

3-Chloropropyl-5-phenyl-3-(trifluoromethyl)-1H-pyrazole-1-carboxylate ***IV-26***. White solid; yield: 63%; m.p. 37.1−37.7 °C; IR (KBr) ν (cm^{-1}): 3061−2853 (C−H), 1748 (O−C═O), 1572 (C═N); ^{1}H NMR (400 MHz, $CDCl_3$) δ (ppm): 7.84−6.49 (m, 6H, Ar−H), 4.61 (t, J = 6.2 Hz, 2H, CH_2), 3.74 (t, J = 6.3 Hz, 2H, CH_2), 2.61 (s, 3H, CH_3), 2.35−2.29 (m, 2H, CH_2); ^{13}C NMR (100 MHz, $CDCl_3$) δ (ppm): 154.24, 150.52, 145.51, 131.80, 129.06, 128.65, 128.65, 126.42, 126.42, 107.90, 64.63, 40.86, 31.53, 14.43; HRMS (ESI): calcd for $C_{14}H_{16}ClN_2O_2$ ([M + H$^+$]), 279.0902; found, 279.0900.

3-Chloropropyl-3,5-diphenyl-1H-pyrazole-1-carboxylate ***IV-27***. White solid; yield: 57%; m.p. 143.7−144.7 °C; IR (KBr) ν (cm^{-1}): 3112−2850 (C−H), 1761 (O−C═O), 1567 (C═N); ^{1}H NMR (400 MHz, $CDCl_3$) δ (ppm): 7.98−6.72 (m, 11H, Ar−H), 4.46 (t, J = 6.0 Hz, 2H, CH_2), 3.36 (t, J = 6.4 Hz, 2H, CH_2), 2.09−2.03 (m, 2H, CH_2); ^{13}C NMR (100 MHz, $CDCl_3$) δ (ppm): 154.46, 149.87, 148.07, 131.52, 131.21, 129.28, 129.28, 129.05, 129.05, 128.76,

https://doi.org/10.1021/acs.jafc.1c02221
J. Agric. Food Chem. 2021, 69, 8366−8379

128.76, 128.05, 128.05, 126.51, 126.51, 109.41, 64.79, 40.71, 31.29; HRMS (ESI): calcd for $C_{19}H_{18}ClN_2O_2$ ([M + H$^+$]), 341.1057; found, 341.1051.

3-Chloropropyl-5-phenyl-3-(trifluoromethyl)-1H-pyrazole-1-carboxylate ***IV-28***. White solid; yield: 52%; m.p. 46.8−47.5 °C; IR (KBr) ν (cm^{-1}): 2969−2852 (C−H), 1775 (O−C═O), 1471 (C═N); ^{1}H NMR (400 MHz, $CDCl_3$) δ (ppm): 7.87−7.19 (m, 6H, Ar−H), 4.31 (t, J = 6.0 Hz, 2H, CH_2), 3.64 (t, J = 6.3 Hz, 2H, CH_2), 2.17−2.11 (m, 2H, CH_2); ^{13}C NMR (100 MHz, $CDCl_3$) δ (ppm): 154.90, 153.78, 148.01, 130.18, 129.94, 128.95, 128.95, 126.47, 126.47, 117.79, 111.11, 64.67, 40.66, 31.28; HRMS (ESI): calcd for $C_{14}H_{13}ClF_3N_2O_2$ ([M + H$^+$]), 333.0618; found, 333.0612.

3-Chloropropyl-5-(p-tolyl)-3-(trifluoromethyl)-1H-pyrazole-1-carboxylate ***IV-29***. Light yellow oily liquid; yield: 40%; IR (KBr) ν (cm^{-1}): 3144−2873 (C−H), 1775 (O−C═O), 1473 (C═N); ^{1}H NMR (400 MHz, $CDCl_3$) δ (ppm): 7.31−6.60 (m, 5H, Ar−H), 4.49 (t, J = 6.0 Hz, 2H, CH_2), 3.38 (t, J = 6.4 Hz, 2H, CH_2), 2.42 (s, 3H, CH_3), 2.13−2.07 (m, 2H, CH_2); ^{13}C NMR (100 MHz, $CDCl_3$) δ (ppm): 148.97, 148.83, 145.82, 145.43, 139.92, 126.62, 126.62, 126.62, 121.72, 121.72, 119.03, 65.65, 40.48, 31.16, 21.41; HRMS (ESI): calcd for $C_{15}H_{15}ClF_3N_2O_2$ ([M + H$^+$]), 340.0774; found, 347.0765.

3-Chloropropyl-5-(furan-2-yl)-3-(trifluoromethyl)-1H-pyrazole-1-carboxylate ***IV-30***. Light yellow oily liquid; yield: 35%; IR (KBr) ν (cm^{-1}): 3148−2929 (C−H), 1780 (O−C═O), 1507 (C═N); ^{1}H NMR (400 MHz, $CDCl_3$) δ (ppm): 7.47−6.46 (m, 4H, Ar−H), 4.55 (t, J = 6.1 Hz, 2H, CH_2), 3.58 (t, J = 6.2 Hz, 2H, CH_2), 2.23−2.17 (m, 2H, CH_2); ^{13}C NMR (100 MHz, $CDCl_3$) δ (ppm): 149.01, 144.13, 142.16, 139.15, 121.56, 118.87, 113.98, 111.88, 107.41, 65.92, 40.65, 31.24; HRMS (ESI): calcd for $C_{12}H_{11}ClF_3N_2O_3$ ([M + H$^+$]), 323.0410; found, 323.0409.

1-Chloroethyl-3-methyl-5-phenyl-1H-pyrazole-1-carboxylate ***IV-31***. White solid; yield: 54%; m.p. 132.9−133.8 °C; IR (KBr) ν (cm^{-1}): 3061−2848 (C−H), 1760 (O−C═O), 1573 (C═N); ^{1}H NMR (400 MHz, $CDCl_3$) δ (ppm): 7.77−7.21 (m, 5H, Ar−H), 6.67−6.63 (m, 1H, CH), 6.43 (s, 1H, Ar−H), 2.53 (s, 3H, CH_3), 1.93 (d, J = 5.8 Hz, 3H, CH_3); ^{13}C NMR (100 MHz, $CDCl_3$) δ (ppm): 154.91, 148.46, 145.95, 131.57, 129.27, 128.69, 128.69, 126.54, 126.54, 108.50, 83.81, 25.25, 14.48; HRMS (ESI): calcd for $C_{15}H_{15}ClF_3N_2O_2$ ([M + H$^+$]), 265.0744; found, 265.0741.

Chloroethyl-3,5-diphenyl-1H-pyrazole-1-carboxylate ***IV-32***. White solid; yield: 50%; m.p. 73.6−73.8 °C; IR (KBr) ν (cm^{-1}): 2998−2938 (C−H), 1762 (O−C═O), 1562 (C═N); ^{1}H NMR (400 MHz, $CDCl_3$) δ (ppm): 7.93−6.75 (m, 11H, Ar−H), 6.61−6.57 (m, 1H, CH), 1.72 (d, J = 5.8 Hz, 3H, CH_3); ^{13}C NMR (100 MHz, $CDCl_3$) δ (ppm): 155.08, 148.63, 147.78, 131.32, 130.71, 129.46, 129.23, 129.14, 129.14, 128.78, 128.78, 128.03, 128.03, 126.61, 126.61, 109.88, 83.65, 24.83; HRMS (ESI): calcd for $C_{18}H_{16}ClN_2O_2$ ([M + H$^+$]), 327.0900; found, 327.0892.

1-Chloroethyl-5-phenyl-3-(trifluoromethyl)-1H-pyrazole-1-carboxylate ***IV-33***. White solid; yield: 40%; m.p. 93.7−94.3 °C; IR (KBr) ν (cm^{-1}): 3127−2941 (C−H), 1785 (O−C═O), 1471 (C═N); ^{1}H NMR (400 MHz, $CDCl_3$) δ (ppm): 7.98−7.21 (m, 6H, Ar−H), 6.77−6.73 (m, 1H, CH), 2.01 (d, J = 5.8 Hz, 3H, CH_3); ^{13}C NMR (100 MHz, $CDCl_3$) δ (ppm): 154.35, 146.03, 136.35, 130.13, 128.97, 126.57, 126.57, 120.34, 120.34, 117.66, 111.74, 84.44, 24.99; HRMS (ESI): calcd for $C_{18}H_{16}ClN_2O_2$ ([M + H$^+$]), 319.0461; found, 319.0456.

1-Chloroethyl-5-(p-tolyl)-3-(trifluoromethyl)-1H-pyrazole-1-carboxylate ***IV-34***. White solid; yield: 37%; m.p. 58.9−59.8 °C; IR (KBr) ν (cm^{-1}): 3131−2921 (C−H), 1778 (O−C═O), 1476 (C═N); ^{1}H NMR (400 MHz, $CDCl_3$) δ (ppm): 7.29−6.62 (m, 5H, Ar−H), 6.58−6.54 (m, 1H, CH), 2.43 (s, 3H, CH_3), 1.79 (d, J = 5.8 Hz, 3H, CH_3); ^{13}C NMR (100 MHz, $CDCl_3$) δ (ppm): 149.52, 147.08, 146.42, 140.03, 129.07, 129.07, 128.95, 126.12, 121.61, 118.93, 108.78, 84.17, 24.81, 21.43; HRMS (ESI): calcd for $C_{18}H_{16}ClN_2O_2$ ([M + H$^+$]), 333.0618; found, 333.0612.

1-Chloroethyl-5-(furan-2-yl)-3-(trifluoromethyl)-1H-pyrazole-1-carboxylate ***IV-35***. White solid; yield: 33%; m.p. 41.9−42.5 °C; IR (KBr) ν (cm^{-1}): 3158−2964 (C−H), 1774 (O−C═O), 1507 (C═N); ^{1}H NMR (400 MHz, $CDCl_3$) δ (ppm): 7.49−6.86 (m, 3H, Ar−H), 6.63−6.59 (m, 1H, CH), 6.47 (dd, J = 3.5, 1.8 Hz, 1H, Ar−H), 1.90 (d, J = 5.8 Hz, 3H CH_3); ^{13}C NMR (100 MHz, $CDCl_3$) δ (ppm): 147.21, 144.29, 141.85, 139.71, 121.44, 118.76, 114.39, 111.97, 107.66, 84.50, 25.04; HRMS (ESI): calcd for $C_{18}H_{16}ClN_2O_2$ ([M + H$^+$]), 309.0254; found, 309.0247.

X-ray Diffraction. The crystal of compound **IV-17** with a size of 0.13 mm × 0.12 mm × 0.10 mm was measured at 293(2) K using graphite-monochromated Mo Kα radiation (λ = 0.71073 Å) on a Rigaku R-AXIS-RAPID area-detector diffractometer (Japan). θ_{max} = 25.24, 20,730 measured reflections and 3503 independent reflections (R_{int} = 0.0292) (Figure 1). The crystalline structure was solved with SHELXS 97 direct methods and deposited to the Cambridge Crystallographic Data Centre under Supplementary Publication No. CCDC 2064120.

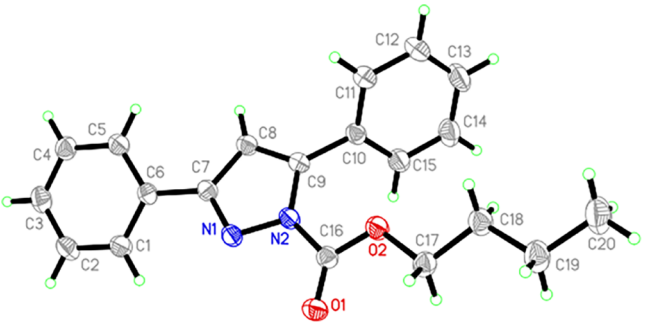

Figure 1. X-ray crystal structure for compound **IV-17**.

Plant Material and Growth Conditions. Wheat seeds (College of Agriculture, Northeast Agricultural University, Harbin, China) were soaked in warm water for 0.5 h. Next, the samples were soaked in 0.6% carbendazim for approximately 0.5 h. The seeds were then washed with distilled water; afterward, the seeds were soaked in the title compounds (10 mg/kg) for 12 h. After germination at 26.5 °C for 24 h, 180 g of soil (Northeast Agricultural University, Harbin, China) was placed and sown in paper cups at a density of seven wheat seeds per cup, sprayed with an appropriate amount of water, and covered with 30 g of topsoil. The seeds were then placed in an incubator at 26.5 °C under a 12 h light/12 h dark photoperiod. The stems and leaves were sprayed with 200 g.a.i/hm^2 FE when the seedlings reached the two-leaf stage. Equal volumes of water were sprayed on the control plants. After 7 days of cultivation, the injury recovery rate (IRR) of each growth index (root length, plant height, and root and plant fresh weights) was measured. The injury recovery rate is calculated according to the following equation

$$\text{Injury Recovery Rate (IRR)}(\%) = \frac{\text{treated with safener and FE} - \text{treated with FE}}{\text{contrast} - \text{treated with FE}} \times 100\%$$

GST, CYP450, ACCase Extraction, and Assay *In Vivo*. The Plant GST ELISA Kit, Plant CYP450 ELISA Kit, and Plant ACCase ELISA Kit (Shanghai Enzyme-Linked Biotechnology Co., Ltd.) were used to determine the activities of GST and CYP450 and the content of ACCase, respectively. All the experiments were performed at 0−4 °C. First, 0.1 g of the wheat root or leaf tissue was put into the mortar after being washed with distilled water and dried, and a certain amount of PBS (pH = 7.4) was added to the mortar, which was quickly frozen, mashed to a homogenate, poured into a centrifuge tube, and centrifuged for 20 min. The supernatant was carefully collected and used for testing the enzymes. The activities of GST, CYP450, and ACCase were assayed according to the manufacturer's instructions with three duplicates per experiment.

Statistical Analysis. Each reported value represents the mean ± standard deviation (SD) of at least three replicate data points for each measurement method. Three different batches of wheat plants were repeatedly tested for the purpose of determining the growth indexes.

https://doi.org/10.1021/acs.jafc.1c02221
J. Agric. Food Chem. 2021, 69, 8366−8379

Scheme 3. Route for the Synthesis of the Title Compounds

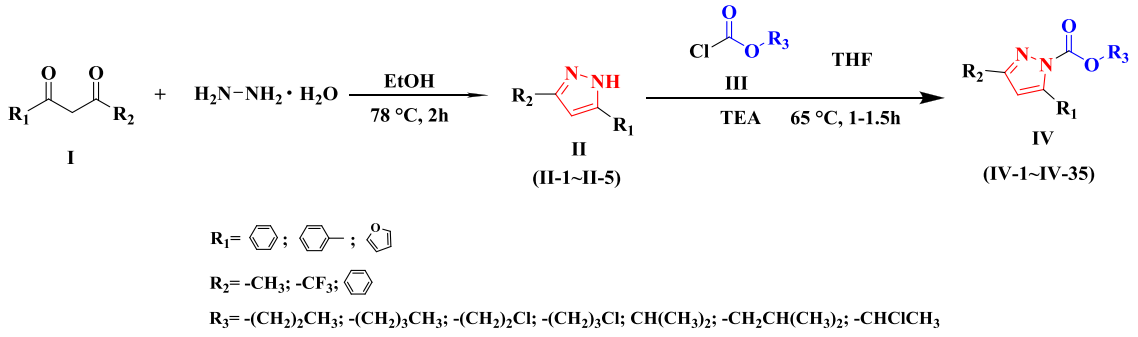

SPSS 20 (IBM Corp., Armonk, NY, USA) was used for the statistical analysis. Through Duncan's tests, significant differences between treatment methods were identified when $p < 0.05$.

Docking Study. The 3D structures of mefenpyr-diethyl, compound **IV-21**, and FA were created in the Sketch module of SYBYL-X 2.0 (Tripos, Inc., St. Louis, MO, USA). The Gasteiger−Hückel charges were computed, and the molecule was further optimized. The crystalline structure of ACCase was downloaded from the Protein Data Bank (PDB ID: 1UYR) and pretreated to repair the main chain, the side chain, and the terminal of the protein to make the structure complete. Molecular docking was then performed using the CDOCKER module in Discovery Studio 3.5 (BIOVIA, Inc., San Diego, CA, USA).[48] Water and a number of other cocrystallized small molecules were eliminated. The protein structure was obtained with the use of the CHARMM force field. The carboxyltransferase (CT) domain of acetyl-CoA carboxylase (ACC) is the site of action of commercial herbicides, such as haloxyfop, diclofop, and sethoxydim. The inhibitors are bound in the active site, i.e., at the interface of the dimer of the CT domain. Inhibitor binding requires large conformational changes for several residues in this interface, which create a highly conserved hydrophobic pocket that extends deeply into the core of the dimer. The active site was defined as a subregion of 13.0 Å from the center of the known ligand. According to the principle of complementary shapes and properties of the receptor and the ligand, a small molecule is placed at the active site to make the ligand and the receptor complementary in shape and nature.[49] The Top Hits parameter was set to 100, and the remaining parameters were default values. The native ligand was redocked to ensure the accuracy of protein preparation. The small molecule−receptor protein complex was evaluated using the interaction energy as an evaluation index.

RESULTS AND DISCUSSION

Chemistry. The synthetic route is outlined in Scheme 3. Key intermediates **II** were obtained by cyclizing 1,3-dione **I** and hydrazine hydrate. It was observed that the solvent substantially affects the product yield. The results indicate that anhydrous ethanol is a better solvent than no solvent or methanol. The corresponding intermediates **II-1** to **II-5** had yields of 73−88% (Table S2).

The synthetic route of compound **IV** is depicted in Scheme 3. With tetrahydrofuran as a solvent, the acid chloride was reacted with intermediate **II** and stirred for 1−1.5 h to obtain compound **IV** (Table S3). The yields of the target compounds **IV-1** to **IV-20** were within the range of 40−87% (Table S3). The R_1 substituent on the pyrazole ring significantly affected the yield of the products. The yields of compounds **IV-11** to **IV-13** (R_1 = phenyl group), **IV-14** (R_1 = benzyl), and **IV-15** (R_1 = furyl) were 87, 82, 78, 70, and 64%, respectively. The target compounds with the six-membered benzene ring structure exhibited better yields than those with the five-membered furan ring. The structure of the six-membered benzene ring is likely to be more stable than that of the five-membered furan ring. This phenomenon might be attributed to the high electronegativity of the O atom in the furan ring, the fact that the electron cloud distribution is not as uniform as that of the benzene ring, and that the conjugation effect is lower than that of the benzene ring. Notably, the introduction of $-CH_3$ on the benzene ring would reduce the yield of compound **IV**. This may be caused by the addition of $-CH_3$ on the benzene ring in the structure, which further increased the steric hindrance and was not conducive to the reaction. The R_2 substituent on the pyrazole ring significantly affected the yields of products. The yields of compounds **IV-11** (R_2 = $-CH_3$), **IV-12** (R_2 = phenyl), and **IV-13** (R_2 = $-CF_3$) were 87, 82, and 78%, respectively. The yield of compounds with $-CH_3$ substituents at R_2 was the highest. The reason for this phenomenon may be that the electron-donating group $-CH_3$ on the ring increased the electron cloud density, which was conducive to the reaction. In contrast, the strong electron-withdrawing group $-CF_3$ substituent on the heterocyclic ring reduces the electron cloud density, leading to a lower yield, and the conjugation effect caused by the benzene ring led to an increased yield. Apparently, the spatial structure of R_3 has a significant impact on the yield of the products. In general, the yield of the linear chain structure is essentially higher than that of the branched chain structure. The yields of compounds **IV-1**, **IV-6**, **IV-11**, and **IV-16** were 73, 70, 87, and 81%, respectively.

The yields of compounds **IV-21** to **IV-35** ranged from 33 to 65% (Table S3). It could be observed that the conclusion obtained from the yields of compounds **IV-1** to **IV-20** were also applicable to the yields of compounds **IV-21** to **IV-35**. The yields of compounds **IV-35** and **IV-21** were 33 and 65%, respectively, which were lower than those of compounds **IV-5** and **IV-11**, which were 47 and 87%, respectively. This may be because the addition of Cl atoms might significantly increase the volume of the acid chloride, and the excessive steric hindrance impeded the reaction, resulting in a decrease in the acid chloride reaction activity. Meanwhile, it weakened its electron-withdrawing effect, which made the acyl chloride carbonyl carbon less positively charged. The C−Cl bond of the acyl portion was difficult to break, which led to a decrease in the yield. The results showed that due to the introduction of the Cl atom on R_3 into the structure, the yields of compounds **IV-11** to **IV-35** were lower than those of compounds **IV-1** to **IV-20**. On the whole, the highest yields were obtained when R_1 and R_2 were replaced by the benzene ring and $-CH_3$, with the introduction of a benzyl or furyl on R_1 and $-CF_3$ or a phenyl on R_2 reducing the yields. The yield of the linear chain structure on R_3 is essentially higher than that of the branched chain structure (Figure 2).

https://doi.org/10.1021/acs.jafc.1c02221
J. Agric. Food Chem. 2021, 69, 8366−8379

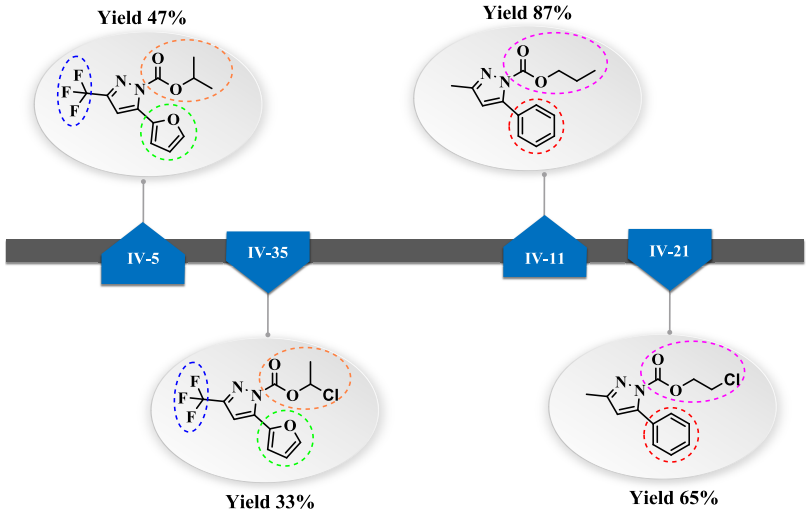

Figure 2. Structure and yield comparison of final products **IV-5**, **IV-35**, **IV-11**, and **IV-21**.

Table 1. Protective Effect of Target Compounds on the Growth Indexes of Wheat[a,b,c]

compound	root length IRR (%)	plant height IRR (%)	root fresh weight IRR (%)	plant fresh weight IRR (%)
mefenpyr-diethyl	79.15 ± 1.53a	97.87 ± 1.76abc	116.15 ± 2.01a	79.15 ± 1.54a
IV-1	60.99 ± 0.72cde	69.78 ± 0.56ef	123.17 ± 1.95a	69.57 ± 0.78b
IV-2	30.49 ± 0.34fgh	83.02 ± 0.54cd	65.88 ± 0.42ef	1.33 ± 0.12gh
IV-3	51.52 ± 0.32e	124.47 ± 1.31a	74.69 ± 0.97de	57.29 ± 0.47cd
IV-4	36.80 ± 0.17fg	103.49 ± 0.92abc	108.98 ± 1.42a	66.93 ± 0.65bc
IV-5	9.42 ± 0.26h	88.16 ± 0.72cd	7.17 ± 0.15h	−4.15 ± 0.19h
IV-6	65.98 ± 0.92c	60.95 ± 0.78ef	99.43 ± 1.03abc	78.34 ± 0.78a
IV-7	57.08 ± 0.81de	27.34 ± 0.29g	57.32 ± 0.82f	14.33 ± 0.23g
IV-8	34.78 ± 0.45fg	98.34 ± 1.04bc	71.23 ± 0.74de	56.78 ± 1.57cd
IV-9	53.78 ± 0.89e	101.67 ± 2.62abc	85.94 ± 1.86cd	61.23 ± 1.08bcd
IV-10	21.06 ± 0.41gh	106.23 ± 3.17ab	00.21 ± 0.06h	10.43 ± 0.37g
IV-11	75.26 ± 1.68ab	80.32 ± 1.83cde	103.20 ± 3.63abc	61.00 ± 1.46bcd
IV-12	56.82 ± 2.68de	102.34 ± 1.46ab	74.26 ± 0.93de	36.17 ± 0.52def
IV-13	80.97 ± 1.16a	93.46 ± 1.36bcd	99.64 ± 2.49abc	50.27 ± 1.85cde
IV-14	59.96 ± 1.03cde	98.23 ± 1.49abc	80.97 ± 2.14cde	61.69 ± 0.82bcd
IV-15	40.49 ± 0.72ef	93.22 ± 0.81bcd	96.91 ± 1.90abc	55.96 ± 1.38cd
IV-16	69.05 ± 1.65bc	71.36 ± 1.27de	106.42 ± 1.97ab	69.34 ± 0.93b
IV-17	43.97 ± 1.08ef	69.78 ± 1.95ef	92.03 ± 0.69bcd	35.23 ± 0.25def
IV-18	55.09 ± 0.51de	72.07 ± 0.74bc	97.87 ± 1.02abc	65.34 ± 0.64bc
IV-19	63.87 ± 0.76cd	69.23 ± 0.61bc	69.78 ± 0.75ef	51.44 ± 0.36cde
IV-20	12.65 ± 0.15h	54.42 ± 0.52de	83.02 ± 0.72cd	71.57 ± 0.89ab
IV-21	86.80 ± 0.36a	95.01 ± 0.46a	124.47 ± 0.82a	85.43 ± 0.61a
IV-22	42.06 ± 0.41ef	55.82 ± 0.31de	103.49 ± 1.31abc	62.04 ± 0.35bcd
IV-23	64.14 ± 0.74cd	68.69 ± 0.73bc	88.16 ± 0.74cd	65.16 ± 0.62bc
IV-24	81.48 ± 1.38a	85.80 ± 0.83ab	60.95 ± 0.65ef	78.23 ± 0.92a
IV-25	−47.32 ± 0.46i	40.34 ± 0.73ef	27.34 ± 0.27g	49.34 ± 0.52de
IV-26	73.56 ± 0.53bc	67.87 ± 0.92bcd	98.34 ± 1.04bc	76.34 ± 0.73a
IV-27	40.97 ± 0.83efg	61.23 ± 0.98cde	101.67 ± 1.75abc	57.24 ± 0.74cd
IV-28	56.97 ± 0.59de	69.87 ± 0.86bc	106.23 ± 1.07ab	60.34 ± 0.86bcd
IV-29	72.05 ± 0.57ab	41.56 ± 0.78ef	80.32 ± 0.64cde	49.34 ± 0.29de
IV-30	26.98 ± 0.38gh	64.32 ± 0.91cd	102.34 ± 1.40ab	64.23 ± 0.41bc
IV-31	51.02 ± 0.53e	27.08 ± 0.36gh	93.46 ± 1.04bcd	43.45 ± 0.62def
IV-32	34.54 ± 0.46fg	40.67 ± 0.61ef	98.23 ± 1.77abc	54.45 ± 0.85cde
IV-33	49.56 ± 0.70ef	51.67 ± 0.58de	93.22 ± 1.64bcd	56.43 ± 0.45cd
IV-34	40.21 ± 0.63efg	15.68 ± 0.16h	71.36 ± 0.62de	36.23 ± 0.36def
IV-35	−15.43 ± 0.31i	69.23 ± 0.72bc	69.78 ± 0.91ef	51.44 ± 0.68cde

[a]Data are means of three replicates. [b]Water treated was used as contrast. [c]Statistical analyses of the data were conducted using SPSS software, and different lowercase letters in the table indicate significant differences ($p < 0.05$).

https://doi.org/10.1021/acs.jafc.1c02221
J. Agric. Food Chem. 2021, 69, 8366−8379

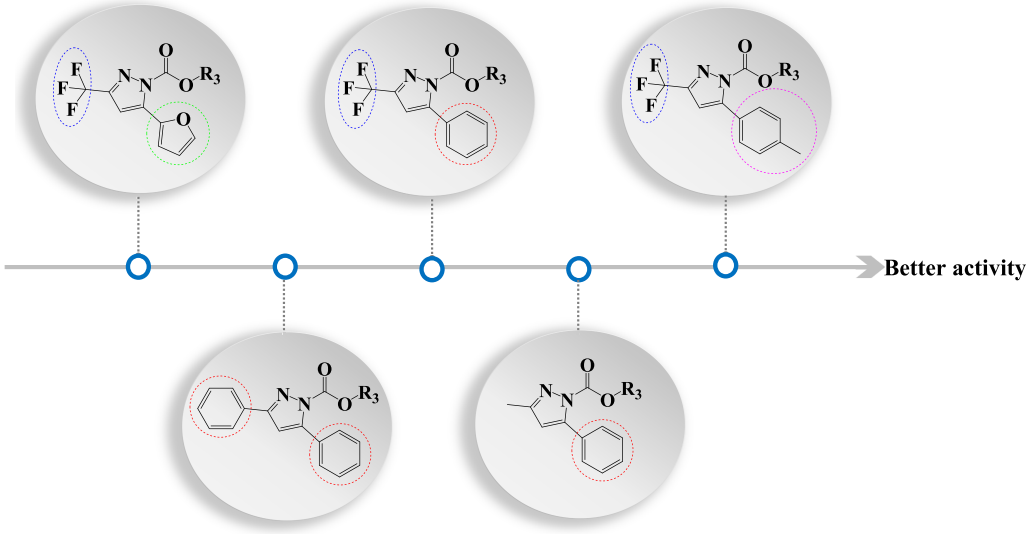

R_3= -$(CH_2)_2Cl$ > -$(CH_2)_3Cl$ > -$CHClCH_3$ > -$(CH_2)_2CH_3$ > -$(CH_2)_3CH_3$ > $CH(CH_3)_2$ > -$CH_2CH(CH_3)_2$

Figure 3. Sequence of activity with different substitutions.

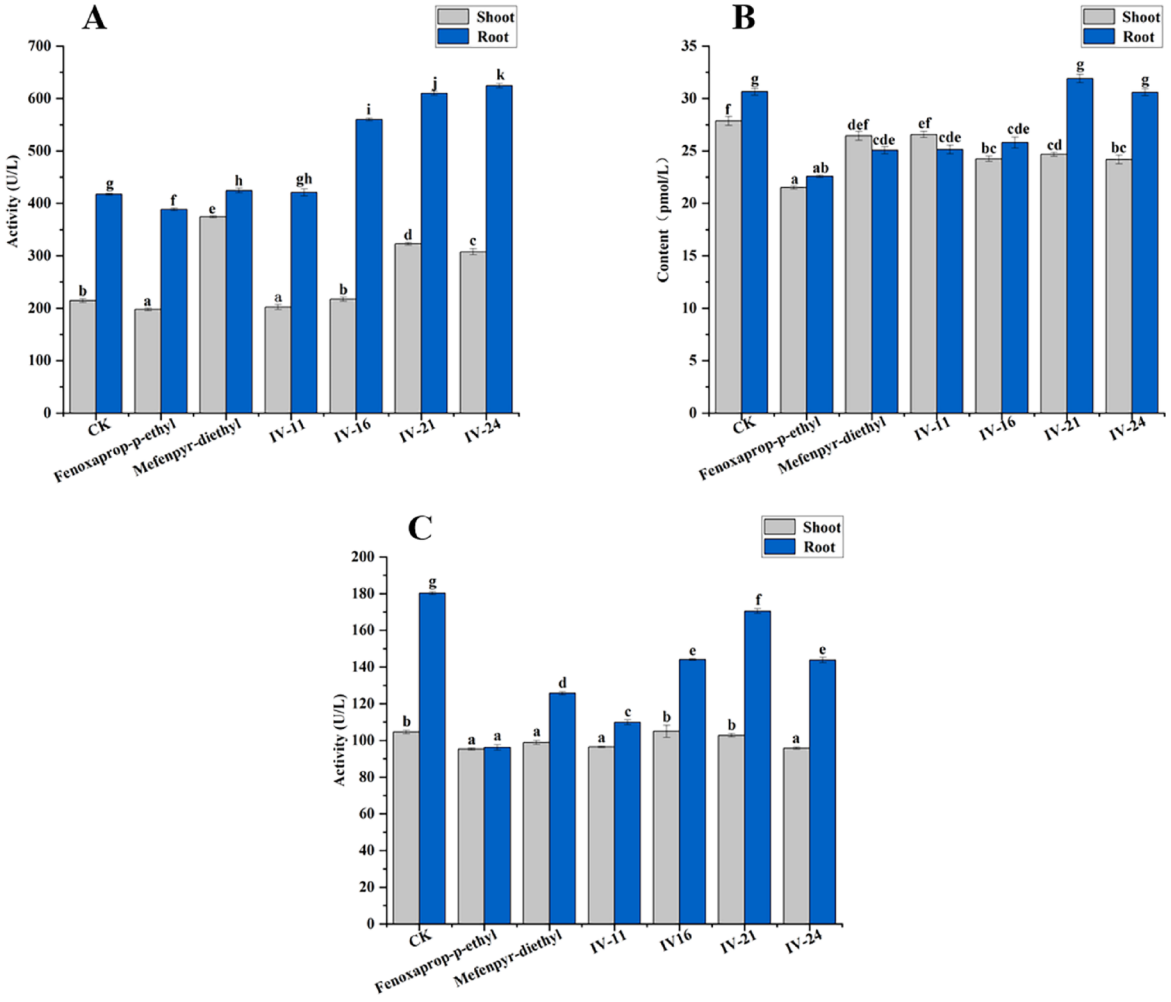

Figure 4. Effect of compounds on GST activity (A), ACCase content (B), and CYP450 activity (C) *in vivo* of wheat.

Biological Activity and Structure–Activity Relationships (SARs). The safener activity of target compound **IV** in a greenhouse was assessed. All new compounds were assessed for their protective effects on wheat *in vivo* against FE damage at a concentration of 200 g/hm^2 (Table 1). It is exciting that most of the compounds presented excellent effects on the

https://doi.org/10.1021/acs.jafc.1c02221
J. Agric. Food Chem. 2021, 69, 8366−8379

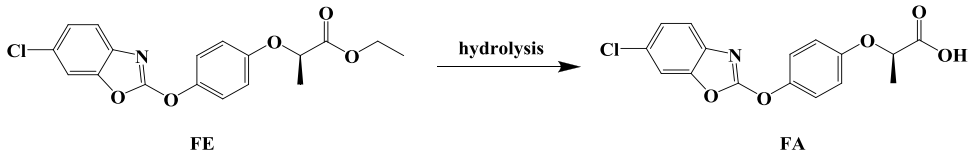

Figure 5. Metabolic hydrolysis of FE.

recovery of the growth index, indicating that the title compounds were successfully designed.

As shown in Table 1, a majority of the title compounds promoted the recovery rate of the growth indexes. Among the rest, compound **IV-21** showed an excellent activity against FE. The IRRs of compound **IV-21** on the root length, plant height, root fresh weight, and plant fresh weight were 86.80, 124.47, 95.01, and 85.43%, respectively, which demonstrates that compound **IV-21** is even better than mefenpyr-diethyl. Notably, diverse biological activities were presented by different substituents. For the same replacement in R_3, the compounds with other substitutions that had phenyl at the R_1 position showed an excellent biological activity compared with those with furyl at the R_1 position. For example, the recovery rate of the root length of compound 4(S3) was 5.5 times higher than that of its corresponding compound **IV-5**. Compounds with the electron-donating group $-CH_3$ at R_2 showed a higher safener biological activity than that of the structure with the strong electron-withdrawing group $-CF_3$. For instance, the IRR of root fresh weight was just 88.16% for compound **IV-23** (R_2 = $-CF_3$), while it was 124.47% for compound **IV-21** (R_2 = $-CH_3$). Obviously, the target compounds with diverse substitutions of the ester had a significant impact on the biological activity. Target compound **IV** with a Cl atom at R_3 showed an excellent biological activity compared with the corresponding structure with an alkyl. For example, recoveries of the root length in the case of compounds **IV-21** and **IV-29** were 86.80 and 72.05%, which were better than those in the case of compounds **IV-11** and **IV-19**, with 75.26 and 63.87%, respectively. Based on the overall biological activity, the chlorine atom may increase the activity of the target compounds.

In summary, the SAR at R_1 can be briefly summarized as follows (Figure 3): phenyl > benzyl > furyl. The biological activity was obtained when R_2 was replaced by $-CH_3$, which was essentially higher than that of $-CF_3$. The safener activity of the linear chain structure on R_3 is essentially higher than that of the branched chain structure, and introduction of the Cl atom increased the safener activity. The SAR results indicated that the structure of compound **IV-21** showed a greater similarity to mefenpyr-diethyl. This indicated that the structure−activity correlations could be used to determine the bioactivity, as they provided valuable information about the required substituents for biological activity.

GST Activity. GST, present in a plant from the early embryonic stage to the mature stage, plays a significant role in the process of herbicide detoxification and protects the plant from oxidative damage.[50−53] To further explore the specific influence of compound **IV** on GST activity, compounds **IV-11**, **IV-16**, **IV-21**, and **IV-24** with a better bioactivity were singled out. Next, their detoxification mechanisms were further explored, and the commercialized safener mefenpyr-diethyl was used as a control.

The results of the enzyme assay showed that the activity of GST in wheat treated with FE was 388.52 U/L in roots and 197.71 U/L in the shoot protein, which were lower than those in CK (Figure 4). These results prove that the GST activity of wheat could be decreased by FE. As shown in Figure 4, obvious enhancements in the GST activity by 374.38, 202.10, 217.27, 322.80, and 307.61 U/L in shoots and 424.41, 421.12, 560, 610.21, and 624.49 U/L in roots were found after treatment with mefenpyr-diethyl and compounds **IV-11**, **IV-16**, **IV-21**, and **IV-24**, respectively. The GST activity was obviously increased, and the induction rate was 197.71 U/L in shoots and 388.52 U/L in roots after treatment with FE. Apparently, the promotion of GST in the wheat root and shoot tissues after pretreatment with FE was lower than that after treatment with the target compounds. From the above conclusions, it can be indicated that the four test compounds showed excellent protective effects and raised the tolerance of wheat to FE by enhancing the GST activity. Among these compounds, compound **IV-21** had the best effect and achieved GST activities of 610.21 U/L in roots and 332.8 U/L in shoots, which were even better than those of mefenpyr-diethyl. To further explore the protection mechanism of the compounds, the ACCase content and CYP450 activity assays of these four compounds were determined.

ACCase Content. FE is an ACCase inhibitor, provoking significant chlorosis and growth inhibition in wheat. The ACCase content *in vivo* was measured to verify the influence of the synthesized compound on the target enzyme of the herbicide. Compounds **IV-11**, **IV-16**, **IV-21**, and **IV-24**, with good safener activities, were selected to detect the ACCase content based on the bioassay test. Mefenpyr-diethyl was used as a control.

As shown in Figure 4, the contents of ACCase in wheat treated with FE were 24.58 pmol/L in roots and 23.51 pmol/L in shoots, which were lower than those in CK. The content of ACCase was obviously decreased by FE. It was found that the ACCase content was recovered after treatment with compounds **IV-11**, **IV-16**, **IV-21**, and **IV-24**, similar to mefenpyr-diethyl. The contents of ACCase in wheat treated with **IV-11** were 25.14 pmol/L in roots and 26.57 pmol/L in shoots, which were higher than those in wheat treated with mefenpyr-diethyl. Among them, compound **IV-21** recovered the ACCase content to the CK level, with its content in the roots reaching 31.91 pmol/L. In general, all the selected compounds interfered with the inhibition of ACCase *via* FE.

CYP450 Activity. CYP450 is a key enzyme in the metabolism of herbicides, and safeners work through the induction of enzyme systems. Compounds **IV-11**, **IV-16**, **IV-21**, and **IV-24** were selected, and mefenpyr-diethyl was used as a control. The CYP450 activity of wheat was measured, and the results are shown in Figure 4.

The four test compounds increased the CYP450 activity of wheat. Compounds **IV-16** and **IV-21** showed a better effect *in vivo* than mefenpyr-diethyl. Compound **IV-21** was the most effective, with CYP450 activities of 170.47 and 102.85 U/L in roots and in shoots, respectively. The effects of compound **IV-11** were weak. The results of the comprehensive effects of

https://doi.org/10.1021/acs.jafc.1c02221
J. Agric. Food Chem. 2021, 69, 8366−8379

Table 2. Chemical Property Comparisons of FA, Mefenpyr-diethyl, and Compound IV-21

	FA	mefenpyr-diethyl	compound **IV-21**
Structure	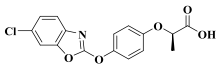	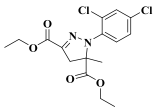	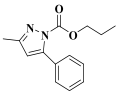
Interaction Energy (kcal/mol)[a]	-30.07	-26.63	-26.73
MW[a]	333.72	373.23	264.71
Log*p*[a]	4.071	4.077	3.667
HBAs[a]	5	6	3
HBDs[a]	1	0	0
RBs[a]	5	7	4
Ars[a]	3	1	2
SA[a]	311.17	370.33	265.70
electronegativity[b]	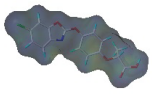	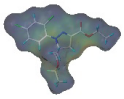	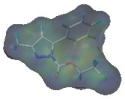

[a]Discovery Studio 3.5 for interaction energy, MW, log *p*, rotatable bonds (RBs), aromatic rings (ARs), and surface area (SA). [b]Electronegativity was predicted using SYBYL-X 2.0 (Tripos, Inc., St. Louis, MO, USA).

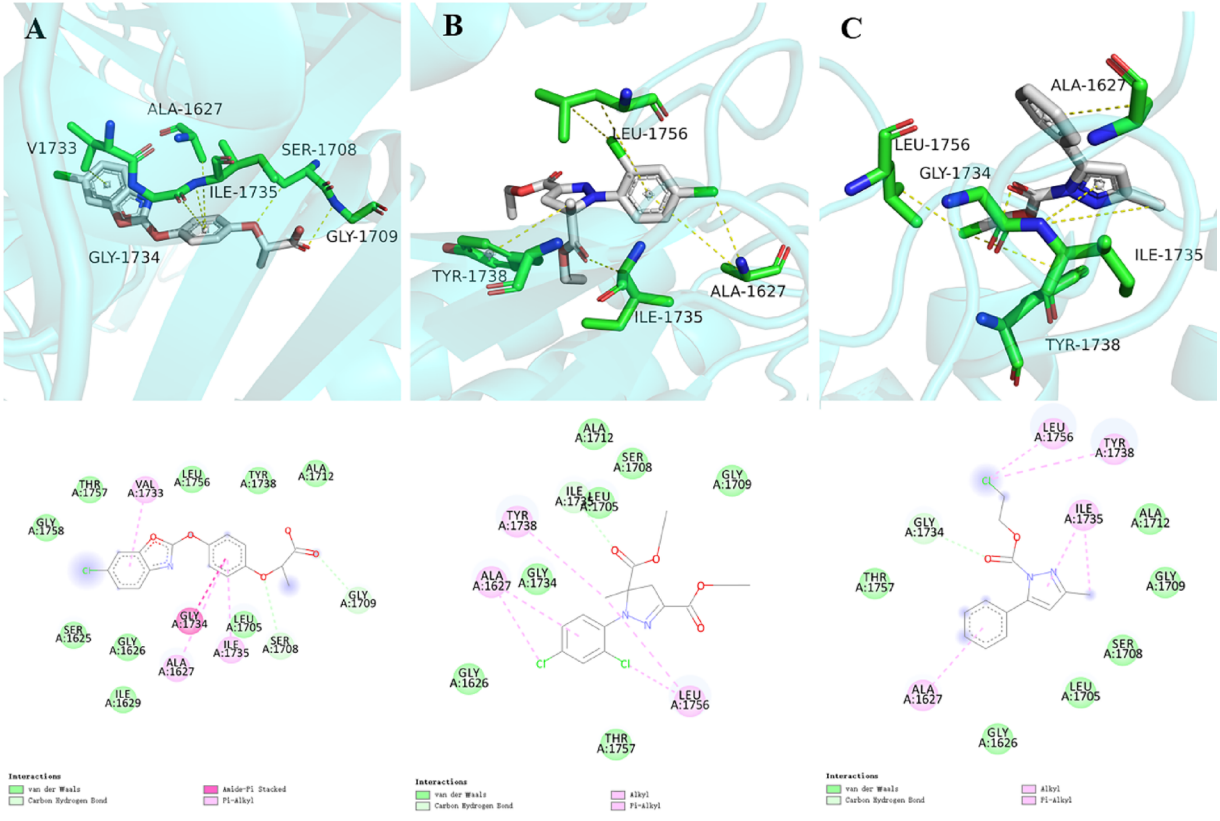

Figure 6. Receptor−ligand interactions of FA (A), mefenpyr-diethyl (B), and compound **IV-21** (C) with the active site of ACCase.

https://doi.org/10.1021/acs.jafc.1c02221
J. Agric. Food Chem. 2021, 69, 8366−8379

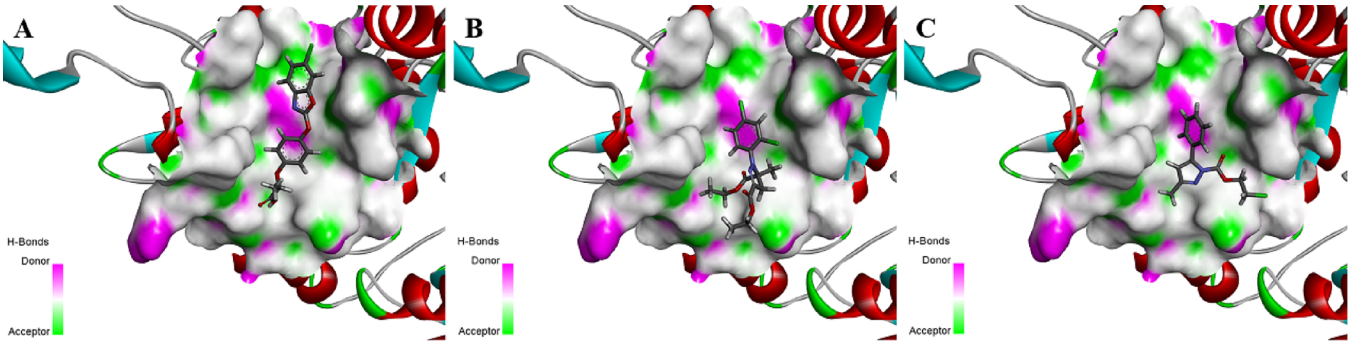

Figure 7. Docking modeling of FA (A), mefenpyr-diethyl (B), and compound **IV-21** (C) with ACCase.

safeners on the GST activity and ACCase content showed that safeners induced GST activity and the ACCase content in plants and increased the CYP450 activity in wheat.

Molecular Structure Comparisons. The pharmacological activity and its interaction with the target enzyme of the compounds are greatly affected by the physicochemical properties. The similar property principle (SPP) refers to the fact that molecules share similar structures, display similar properties, and use similar binding modes when molecules interact with the target proteins.[54,55] FE is hydrolyzed into the corresponding acid in plants; here, FA is selected as the structure for comparison (Figure 5).[49] By comparing the physicochemical properties of compound **IV-21**, mefenpyr-diethyl, and FA (Table 2), it is not difficult to see that the log *p*, hydrogen-bond donors (HBDs), aromatic rings (ARs), surface area (SA), and electronegativity of the three compounds had a strong resemblance. In addition, more hydrogen-bond acceptors (HBAs) were found in mefenpyr-diethyl. The molecular weight (MW) of compound **IV-21** was relatively low, which was conducive to the metabolism of exogenous compounds for crops. The rotatable bonds (RBs) of compound **IV-21** were lower than those of mefenpyr-diethyl, which could allow for the dominant conformation to be successfully locked and was conducive to the efficacy of the drug. This finding indicated that compound **IV-21** has enormous potential to become the leading structure of new herbicide safeners.

Molecular Docking. Molecular docking is considered to be a highly efficient method for predicting the interactions between ligands and receptors.[56] To further verify the detoxification mechanism of safeners on wheat, a molecular docking study was performed to confirm the interactions between the active compounds and ACCase.

The crystalline structure of ACCase (PDB ID: 1UYR) was used to carry out the molecular docking experiment. As shown in Figure 6, FA interacted with six amino acid residues, of which Gly 1734 formed amide−π stacked interactions with the phenyl of FA. Moreover, FA formed π−alkyl interactions with Val 1627, Val 1733, and Ile 1735. There were also alkyl and π−alkyl nonpolar interactions between compound **IV-21** and Ala 1627, Ile 1735, Leu 1756, and Tyr 1738. It was clear that compound **IV-21** formed an additional π−alkyl interaction with Ile 1735 compared to mefenpyr-diethyl. Therefore, the mechanism of compound **IV-21** is similar to that of mefenpyr-diethyl, except that compound **IV-21** bonds are more stable with ACCase. Although there are more HBAs in mefenpyr-diethyl, HBAs hardly affect the interaction in the active site. By comparing the interaction energy of the three compounds, it was not difficult to see that the interaction energy of FA was 30.07 kcal/mol, which was higher than those of mefenpyr-diethyl and compound **IV-21** (Table 2), which indicated that the binding of FA and ACCase was stronger than that of the other two compounds. It was thus speculated that both compound **IV-21** and mefenpyr-diethyl interacted with the amino residues in the active site of ACCase, which hindered herbicide insertion.

Furthermore, geometric matching models were established (Figure 7). FA was well-embedded in the active pocket, filling the entire active pocket and acting on multiple amino acid sites, thereby causing the inhibition effect. Notably, neither mefenpyr-diethyl nor compound **IV-21** matched well in terms of spatial geometry as FA did, so it could not exert a similar weed control effect. However, mefenpyr-diethyl and compound **IV-21** occupied part of the active site. This prevented FA from reaching or acting with ACCase when compound **IV-21** was applied before or with an herbicide.

ADMET Prediction. Many drugs have failed to enter the market due to their toxicity. The pharmacokinetic properties of the active compounds are predicted in Table 3. The solubility level, absorption level, and plasma protein binding (PPB# prediction) of the three compounds were exactly analogical. The PPB ability was less than 90%, indicating that mefenpyr-diethyl, compound **IV-21**, and FA bear good bioavailability and would not attach to the carrier protein. Notably, the CYP2D6 prediction showed no inhibition of the CYP2D6 enzyme *via* compound **IV-21**, indicating that it could pass through the first stage of metabolism smoothly, while mefenpyr-diethyl inhibited the CYP2D6 enzyme, and metabolism was easily blocked. In summary, compound **IV-21**

Table 3. ADMET Prediction of FA, Mefenpyr-diethyl, and Compound IV-21

	FA	mefenpyr-diethyl	compound **IV-21**
solubility level[a]	2	2	2
absorption level[b]	0	0	0
CYP2D6 prediction[c]	false	true	false
AlogP98[d]	4.071	3.951	3.664
PPB# prediction[e]	true	true	true

[a]Solubility level: categorical solubility level. 2: Yes, low. [b]Absorption level: absorption level. 0: Good absorption. [c]CYP2D6: cytochrome P450 2D6. <0.161: False, noninhibitor; >0.161: true, inhibitor. [d]AlogP98: the logarithm of the partition coefficient between *n*-octanol and water. <4.0: Binding is <90%; >4.0: binding is >90% and binding is <95%. [e]PPB: plasma protein binding ability. <−2.209: ≥90%, False; > −2.209: ≤90%, true.

https://doi.org/10.1021/acs.jafc.1c02221
J. Agric. Food Chem. 2021, 69, 8366−8379

exhibited better pharmacokinetic properties than mefenpyr-diethyl.

In conclusion, a sequence of new ester-substituted pyrazole derivatives was designed and synthesized based on the fragment splicing method. The bioactivity assay showed that the safening activity was possessed by most of the target compounds, to some extent, preventing wheat from FE injury. Compound **IV-21** showed the greatest activity against FE and enhanced the tolerance of wheat by recovering the ACCase content and enhancing the GST and CYP450 activities. The molecular structure comparisons and molecular docking results indicated that the better bioactivity of compound **IV-21** came from the occupation in the active site of ACCase. The ADMET prediction revealed that compound **IV-21** exhibited excellent pharmacokinetic properties. This information indicated that the ester-substituted pyrazole is a potent safener skeleton to be further optimized and developed.

■ ASSOCIATED CONTENT

Supporting Information

The Supporting Information is available free of charge at https://pubs.acs.org/doi/10.1021/acs.jafc.1c02221.

Materials and manufacturers (Table S1); structures and yields of intermediates **II-1**−**II-5** (Table S2); structures and yields of compounds **IV-1**−**IV-35** (Table S3); detailed analytical IR, ^{1}H NMR, ^{13}C NMR, and HRMS spectra of compounds **IV-1**−**IV-35** (PDF)

■ AUTHOR INFORMATION

Corresponding Authors

Ying Fu − *Department of Chemistry, College of Arts and Sciences, Northeast Agricultural University, Harbin 150030, China;* orcid.org/0000-0003-4265-6879; Phone: +86-451-55190070; Email: fuying@neau.edu.cn

Fei Ye − *Department of Chemistry, College of Arts and Sciences, Northeast Agricultural University, Harbin 150030, China;* orcid.org/0000-0002-7731-752X; Phone: +86-451-55191507; Email: yefei@neau.edu.cn

Authors

Ling Jia − *Department of Chemistry, College of Arts and Sciences, Northeast Agricultural University, Harbin 150030, China*

Shuang Gao − *Department of Chemistry, College of Arts and Sciences, Northeast Agricultural University, Harbin 150030, China;* orcid.org/0000-0003-2012-8768

Yuan-Yuan Zhang − *Department of Chemistry, College of Arts and Sciences, Northeast Agricultural University, Harbin 150030, China*

Li-Xia Zhao − *Department of Chemistry, College of Arts and Sciences, Northeast Agricultural University, Harbin 150030, China*

Complete contact information is available at: https://pubs.acs.org/10.1021/acs.jafc.1c02221

Author Contributions

#L.J. and S.G. contributed equally to this work.

Notes

The authors declare no competing financial interest.

■ ACKNOWLEDGMENTS

This work was supported by the National Nature Science Foundation of China (31572042 and 31801784) and the Natural Science Foundation of Heilongjiang Province (ZD2017002).

■ REFERENCES

(1) Tong, L.; Harwood, H. J. Acetyl-coenzyme A carboxylases: Versatile targets for drug discovery. *J. Cell. Biochem.* **2006**, *99*, 1476−1488.

(2) Tomassetti, M.; Garavaglia, B. S.; Vranych, C. V.; Gottig, N.; Ottado, J.; Gramajo, H.; Diacovich, L. 3-methylcrotonyl Coenzyme A (CoA) carboxylase complex is involved in the Xanthomonas citri subsp citri lifestyle during citrus infection. *PLoS One* **2018**, *13*, No. e0198414.

(3) Keereetaweep, J.; Liu, H.; Zhai, Z.; Shanklin, J. Biotin attachment domain-containing proteins irreversibly inhibit acetyl CoA carboxylase. *Plant Physiol.* **2018**, *177*, 208−215.

(4) Huerlimann, R.; Heimann, K. Comprehensive guide to acetyl-carboxylases in algae. *Crit. Rev. Biotechnol.* **2013**, *33*, 49−65.

(5) Xiang, S.; Callaghan, M. M.; Watson, K. G.; Tong, L. A different mechanism for the inhibition of the carboxyltransferase domain of acetyl-coenzyme A carboxylase by tepraloxydim. *Proc. Natl. Acad. Sci. U. S. A.* **2009**, *106*, 20723−20727.

(6) Wang, J.; Peng, Y.; Chen, W.; Yu, Q.; Bai, L.; Peng, L. The Ile-2041-Val mutation in the ACCase gene confers resistance to clodinafop-propargyl in American sloughgrass (Beckmannia syzigachne Steud). *Pest Manage. Sci.* **2021**, *77*, 2425−2432.

(7) Zhao, N.; Yan, Y.; Ge, L.; Zhu, B.; Liu, W.; Wang, J. Target site mutations and cytochrome P450s confer resistance to fenoxaprop-*P*-ethyl and mesosulfuron-methyl in Alopecurus aequalis. *Pest Manage. Sci.* **2019**, *75*, 204−214.

(8) Chen, G.; Xu, H.; Zhang, T.; Bai, C.; Dong, L. Fenoxaprop-*P*-ethyl resistance conferred by cytochrome P450s and target site mutation in Alopecurus japonicas. *Pest Manage. Sci.* **2018**, *74*, 1694−1703.

(9) Délye, C.; Zhang, X.-Q.; Michel, S.; Matéjicek, A.; Powles, S. B. Molecular bases for sensitivity to acetyl-coenzyme a carboxylase inhibitors in black-grass. *Plant Physiol.* **2005**, *137*, 794−806.

(10) Lancaster, Z. D.; Norsworthy, J. K.; Scott, R. C. Sensitivity of grass crops to low rates of quizalofop. *Weed Technol.* **2018**, *32*, 304−308.

(11) Laforest, M.; Soufiane, B.; Simard, M.-J.; Obeid, K.; Page, E.; Nurse, R. E. Acetyl-CoA carboxylase overexpression in herbicide-resistant large crabgrass (Digitaria sanguinalis). *Pest Manage. Sci.* **2017**, *73*, 2227−2235.

(12) Mccullough, P. E.; Yu, J.; Raymer, P. L.; Chen, Z. First report of ACCase-Resistant goosegrass (Eleusine indica) in the United States. *Weed Sci.* **2016**, *64*, 399−408.

(13) Saini, R. K.; Malone, J.; Gill, G.; Preston, C. Inheritance of evolved clethodim resistance in Lolium rigidum populations from Australia. *Pest Manage. Sci.* **2017**, *73*, 1604−1610.

(14) Tind, T.; Mathiesen, T. J.; Jensen, J. E.; Ritz, C.; Streibig, J. C. Using a selectivity index to evaluate logarithmic spraying in grass seed crops. *Pest Manage. Sci.* **2009**, *65*, 1257−1262.

(15) Papapanagiotou, A. P.; Kaloumenos, N. S.; Eleftherohorinos, I. G. Sterile oat (Avena sterilis L.) cross-resistance profile to ACCase-inhibiting herbicides in Greece. *Crop Prot.* **2012**, *35*, 118−126.

(16) Shen, C.; Tang, W.; Zeng, D.; Xu, H.; Sun, W.; Wu, R. Isoxadifen-Ethyl derivatives protect rice from fenoxaprop-*P*-ethyl-associated injury during the control of weedy rice. *Weed Sci.* **2017**, *65*, 579−587.

(17) Kang, T.; Gao, S.; Zhao, L.-X.; Zhai, Y.; Ye, F.; Fu, Y. Design, synthesis and SAR of novel 1,3-disubstituted imidazolidine or hexahydropyrimidine derivatives as herbicide safeners. *J. Agric. Food Chem.* **2021**, *69*, 45−54.

(18) Wang, Z.-W.; Zhao, L.-X.; Ma, P.; Ye, T.; Fu, Y.; Ye, F. Fragments recombination, design, synthesis, safener activity and

CoMFA model of novel substituted dchloroacetylphenyl sulfonamide derivatives. *Pest Manage. Sci.* **2021**, *77*, 1724−1738.
(19) Elmore, M. T.; Brosnan, J. T.; Armel, G. R.; Vargas, J. J.; Breeden, G. K. Influence of herbicide safeners on creeping bentgrass (agrostis stolonifera) tolerance to herbicides. *Weed Technol.* **2015**, *29*, 550−560.
(20) Casidi, J. E. Pesticide interactions: mechanisms, benefits, and risks. *J. Agric. Food Chem.* **2017**, *62*, 4553−4561.
(21) Del Buono, D.; Terzano, R.; Panfili, I.; Bartucca, M. L. Phytoremediation and detoxification of xenobiotics in plants: herbicide-safeners as a tool to improve plant efficiency in the remediation of polluted environments. A mini-review. *Int. J. Phytorem.* **2020**, *22*, 789−803.
(22) Ye, F.; Zhai, Y.; Guo, K.-L.; Liu, Y.-X.; Li, N.; Gao, S.; Zhao, L.-X.; Fu, Y. Safeners improve maize tolerance under herbicide toxicity stress by increasing the activity of enzymes in vivo. *J. Agric. Food Chem.* **2019**, *67*, 11568−11576.
(23) Riechers, D. E.; Kreuz, K.; Zhang, Q. Detoxification without intoxication: Herbicide safeners activate plant defense gene expression. *Plant Physiol.* **2010**, *153*, 3−13.
(24) Yang, Q.; Li, J.; Shen, J.; Xu, Y.; Liu, H.; Deng, W.; Li, X.; Zheng, M. Metabolic resistance to acetolactate synthase inhibiting herbicide tribenuron-methyl in descurainia sophia L. mediated by cytochrome P450 enzymes. *J. Agric. Food Chem.* **2018**, *66*, 4319−4327.
(25) Taylor, V. L.; Cummins, I.; Brazier-Hicks, M.; Edwards, R. Protective responses induced by herbicide safeners in wheat. *Environ. Exp. Bot.* **2013**, *88*, 93−99.
(26) Brazier-Hicks, M.; Knight, K. M.; Sellars, J. D.; Steel, P. G.; Edwards, R. Testing a chemical series inspired by plant stress oxylipin signalling agents for herbicide safening activity. *Pest Manage. Sci.* **2018**, *74*, 828−836.
(27) Wang, H. C.; Li, J.; Lv, B.; Lou, Y. L.; Dong, L. Y. The role of cytochrome P450 monooxygenase in the different responses to fenoxaprop-*P*-ethyl in annual bluegrass (Poa annua L.) and short awned foxtail (Alopecurus aequalis Sobol.). *Pestic. Biochem. Physiol.* **2013**, *107*, 334−342.
(28) Bolyard, K.; Gresens, S. E.; Ricko, A. N.; Sivey, J. D.; Salice, C. J. Assessing the toxicity of the "inert" safener benoxacor toward chironomus riparuis: effects of agrochemical mixtures. *Environ. Toxicol. Chem.* **2017**, *36*, 2660−2670.
(29) Liu, S.; Deng, X.; Zhou, X.; Bai, L. Assessing the toxicity of three "inter" herbicide safeners toward danio rerio: effects on embryos development. *Ecotox. Environ. Saf.* **2021**, *207*, 111576.
(30) Liu, S.; Deng, X.; Bai, L. Developmental toxicity and transcriptome analysis of zebrafish (danio rerio) embryos following exposure to chiral herbicide safener benoxacor. *Sci. Total Environ.* **2021**, *761*, 143273.
(31) Fu, Y.; Zhang, D.; Kang, T.; Guo, Y.-Y.; Chen, W.-G.; Gao, S.; Ye, F. Fragment splicing-based design, synthesis and safener activity of novel substituted phenyl oxazole derivatives. *Bioorg. Med. Chem. Lett.* **2019**, *29*, 570−576.
(32) Horty, L. G.; Daeuble, J. F.; Castetter, S.; Olson, M. B.; Wessels, F. J.; Wang, N. X. Synthesis, stability and insecticidal activity of 2-arylstilbenes. *Pest Manage. Sci.* **2019**, *75*, 3015−3023.
(33) Li, K.-J.; Qu, R.-Y.; Liu, Y.-C.; Yang, J.-F.; Devendar, P.; Chen, Q.; Niu, C.-W.; Xi, Z.; Yang, G.-F. Design, synthesis, and herbicidal activity of pyrimidine-biphenyl hybrids as novel acetohydroxyacid synthase inhibitors. *J. Agric. Food Chem.* **2018**, *66*, 3773−3782.
(34) Viegas-Junior, C.; Danuello, A.; Bolzani, V. d. S.; Barreir, E. J.; Fraga, C. A. M. Molecular hybridization: A useful tool in the design of new drug prototypes. *Curr. Med. Chem.* **2007**, *14*, 1829−1852.
(35) Guo, K.-L.; Zhao, L.-X.; Wang, Z.-W.; Gao, Y.-C.; Li, J.-J.; Gao, S.; Fu, Y.; Ye, F. Design, synthesis, and bioevaluation of substituted phenyl isoxazole analogues as herbicide safener. *J. Agric. Food Chem.* **2020**, *68*, 10550−10559.
(36) Jeschke, P. Progress of modern agricultural chemistry and future prospects. *Pest Manage. Sci.* **2016**, *72*, 433−455.
(37) Robinson, D. E.; Soltani, N.; Shropshire, C.; Sikkema, P. H. Cyprosulfamide safens isoxaflutole in sweet corn (zea mays L.). *Hortscience* **2013**, *48*, 1262−1265.
(38) Ye, F.; Zhai, Y.; Kang, T.; Wu, S.-L.; Li, J.-J.; Gao, S.; Zhao, L.-X.; Fu, Y. Rational design, synthesis and structure-activity relationship of novel substituted oxazole isoxazole carboxamides as herbicide safener. *Pestic. Biochem. Physiol.* **2019**, *157*, 60−68.
(39) Zhang, Y.-Y.; Gao, S.; Liu, Y.-X.; Wang, C.; Jiang, W.; Zhao, L.-X.; Fu, Y.; Ye, F. Design, synthesis, and biological activity of novel diazabicyclo derivatives as safeners. *J. Agric. Food Chem.* **2020**, *68*, 3403−3414.
(40) Zheng, Y.; Liu, B.; Gou, Z.; Li, Y.; Zhang, X.; Wang, Y.; Yu, S.; Li, Y.; Sun, D. Design of novel CSA analogues as potential safeners and fungicides. *Bioorg. Med. Chem. Lett.* **2015**, *25*, 791−794.
(41) Zhang, Y.-Y.; Gao, S.; Huang, M.-T.; Wang, Z.-W.; Ma, X.; Zhai, Y.; Li, N.; Zhao, L.-X.; Fu, Y.; Ye, F. Protective efficacy of phenoxyacetyl oxazolidine derivatives as safeners against nicosulfuron toxicity in maize. *Pest Manage. Sci.* **2021**, *77*, 177−183.
(42) Li, L.; Gao, S.; Yang, L.; Liu, Y.-L.; Li, P.; Ye, F.; Fu, Y. Cobalt (II) complex as a fluorescent sensing platform for the selective and sensitive detection of triketone HPPD inhibitors. *J. Hazard. Mater.* **2021**, *404*, 124015.
(43) Fu, Y.; Wang, M.; Zao, L.-X.; Zhang, S.-Q.; Liu, Y.-X.; Guo, Y.-Y.; Zhang, D.; Gao, S.; Ye, F. Design, synthesis, herbicidal activity and CoMFA of novel aryl-formyl piperidinone HPPD inhibitors. *Pestic. Biochem. Physiol.* **2021**, *174*, 104811.
(44) Fu, Y.; Zhang, S.-Q.; Liu, Y.-X.; Wang, J.-Y.; Gao, S.; Zhao, L.-X.; Ye, F. Design, synthesis, SAR and molecular docking of novel green niacin-triketone HPPD Inhibitor. *Ind. Crops Prod.* **2019**, *137*, 566−575.
(45) Yang, L.; Liu, Y.-L.; Liu, C.-G.; Ye, F.; Fu, Y. Two luminescent dye@MOFs systems as dual-emitting platforms for efficient pesticides detection. *J. Hazard. Mater.* **2020**, *381*, 120966.
(46) Lee, B.; Kang, P.; Lee, K. H.; Cho, J.; Nam, W.; Lee, W. K.; Hur, N. H. Solid-state and solvent-free synthesis of azines, pyrazoles, and pyridazinones using solid hydrazine. *Tetrahedron Lett.* **2013**, *54*, 1384−1388.
(47) Inkaya, E.; Dincer, M.; Korkusuz, E.; Yildirim, I.; Büyükgüngör, O. Synthesis, spectroscopic characterization and quantum chemical computational studies on 1-acetyl-3,5-di(4-methylphenyl)-1H-pyrazole. *J. Mol. Struct.* **2012**, *1027*, 133−139.
(48) Sakkiah, S.; Thangapandian, S.; John, S.; Kwon, Y. J.; Lee, K. W. 3D QSAR pharmacophore based virtual screening and molecular docking for identification of potential HSP90 inhibitors. *Eur. J. Med. Chem.* **2010**, *45*, 2132−2140.
(49) Zhang, H.; Tweel, B.; Tong, L. Molecular basis for the inhibition of the carboxyltransferase domain of acetyl-coenzyme-A carboxylase by haloxyfop and diclofop. *Proc. Natl. Acad. Sci. U. S. A.* **2004**, *101*, 5910−5915.
(50) Cummins, I.; Dixon, D. P.; Freitag-Pohl, S.; Skipsey, M.; Edwards, R. Multiple roles for plant glutathione transferases in xenobiotic detoxification. *Drug Metab. Rev.* **2011**, *43*, 266−280.
(51) Schröder, P.; Daubner, D.; Maier, H.; Neustifter, J.; Debus, R. Phytoremediation of organic xenobiotics-glutathione dependent detoxification in phragmites plants from european treatment sites. *Bioresour. Technol.* **2008**, *99*, 7183−7191.
(52) Andrews, C. J.; Cummins, I.; Skipsey, M.; Grundy, N. M.; Jepson, I.; Townson, J.; Edwards, R. Purification and characterisation of a family of glutathione transferases with roles in herbicide detoxification in soybean (Glycine max L.); selective enhancement by herbicides and herbicide safeners. *Pestic. Biochem. Physiol.* **2005**, *82*, 205−219.
(53) DeRidder, B. P.; Goldsbrough, P. B. Organ-specific expression of glutathione S-transferases and the efficacy of herbicide safeners in Arabidopsis. *Plant Physiol.* **2006**, *140*, 167−175.
(54) Willett, P. The calculation of molecular structural similarity: principles and practice. *Mol. Inf.* **2014**, *33*, 403−413.
(55) Boström, J.; Hogner, A.; Schmitt, S. Do structurally similar ligands bind in a similar fashion? *J. Med. Chem.* **2006**, *49*, 6716−6725.

https://doi.org/10.1021/acs.jafc.1c02221
J. Agric. Food Chem. 2021, 69, 8366−8379

(56) Dong, Y.; Jiang, X.; Liu, T.; Ling, Y.; Yang, Q.; Zhang, L.; He, X. Structure-based virtual screening, compound synthesis, and bioassay for the design of chitinase inhibitors. *J. Agric. Food Chem.* **2018**, *66*, 3351−3357.

https://doi.org/10.1021/acs.jafc.1c02221
J. Agric. Food Chem. 2021, 69, 8366−8379